Nonleptonic weak decays of charmed baryons

Hai-Yang Cheng
Institute of Physics, Academia Sinica, Taipei, Taiwan 11529, Republic of China

B. Tseng
Physics Department, National Cheng Kung University, Tainan, Taiwan 70101, Republic of China
(Received 10 January 1992)

Two-body nonleptonic weak decays of charmed baryons are analyzed in the framework of the pole model, which is more general and pertinent than current algebra since its use is not restricted to the soft meson limit and to the pseudoscalar-meson final state. The s-wave amplitudes are dominated by the $\frac{1}{2}^-$ baryon resonances. Special attention is paid to the parity-violating $\frac{1}{2}^-$-$\frac{1}{2}^+$ baryon matrix elements, which are evaluated using the MIT bag model. For definiteness, we compute the α asymmetry parameter and the branching ratios for the decay modes $\Lambda_c^+ \to p\bar{K}^0(\bar{K}^{*0})$, $\Lambda\pi^+(\rho^+)$, $\Sigma^0\pi^+(\rho^+)$, $\Sigma^+\pi^0(\rho^0)$, $p\phi$, and find a good agreement with experiment. We conclude that (i) there is no color suppression in $\Lambda_c^+ \to p\bar{K}^0(\bar{K}^{*0})$ and $p\phi$, (ii) nonspectator contributions are in general smaller than the factorizable ones for the decay modes which receive contributions from the factorizable diagram, and (iii) the predicted branching ratios will be too small if the wave functions of the heavy-quark bag model are employed. A comparison of our work with current algebra and other theoretical calculations is made.

PACS number(s): 13.30.Eg, 11.40.Ha, 12.40.Aa, 14.20.Kp

I. INTRODUCTION

Contrary to the significant progress made over the last ten years or so in the studies of the heavy meson decay, advancement in the arena of heavy baryons, both theoretical and experimental, has been very slow [1]. From the theoretical viewpoint, the dynamics of nonleptonic weak decays becomes simpler and simpler as the meson becomes heavier and heavier. For example, the well-known factorization approach has been applied successfully to heavy meson decays. However, the situation is the other way around for the baryon decay: While the hyperon decay can be tackled with the help of current algebra, a rigorous and reliable approach suited for investigating the weak decays of heavy baryons does not exist thus far. This is attributed to the fact that neither current algebra nor the factorization approach is the ultimate tool for analyzing heavy baryon decay.

In the past few years, new and high-statistics measurements of the nonleptonic decay of Λ_c^+ became available. Apart from symmetry considerations [2–5], the phenomenology of two-body nonleptonic decays of charmed baryons is conventionally studied by the technique of current algebra [6–13]. However, the use of this approach is rather limited for the following two reasons. First, the technique of the soft-meson theorem works only if the two-body decay consists of a baryon plus a pseudoscalar meson ($B_c \to BP$); decay modes with a vector-meson final state are beyond the realm of current algebra. Second, the pseudoscalar-meson final state in charmed baryon decay is far from being "soft." This is particularly true in bottom and top baryon decays. Consequently, it is no longer justified to assert that the s-wave amplitude is dominated by the commutator terms and the p-wave amplitude arises from the ground-state pole terms. On the other extreme, weak decays of heavy baryons, e.g., $\Lambda_b \to \Lambda_c \pi(\rho), \Lambda_c D_s$, have been recently investigated using the heavy-quark approximation and the factorization assumption [14]. An important question which must be addressed is whether nonfactorizable contributions are negligible compared to the factorizable ones. This issue together with the aforementioned problems with current algebra calls for a systematic approach for describing heavy-baryon weak decays.

In the present paper we adopt an old-fashioned approach, namely, the pole model in which the baryon decay amplitude is approximated by baryon- and meson-pole contributions, including resonances and continuum states. In general, nonfactorizable s- and p-wave amplitudes are dominated by $\frac{1}{2}^-$ low-lying baryon resonances and $\frac{1}{2}^+$ ground-state intermediate states, respectively, while factorizable amplitudes receive contributions from meson poles. Evidently, the estimate of the s-wave terms in the pole model is a difficult and nontrivial task since it involves weak baryon matrix elements and strong coupling constants of $\frac{1}{2}^-$ baryon states. However, the calculation of the s waves is greatly simplified in the light strange baryon (i.e., hyperon) decay where it is appropriate to take the soft-meson limit. The parity-violating pole amplitude of the hyperon decay is reduced, in the soft pion limit, to the familiar equal-time commutator terms, which are much easier to handle. (In current algebra, the p-wave amplitude is represented by baryon poles for $B \to B' + A_\mu$.) However, this simplification is no longer applicable to heavy-baryon weak decays. The merit of the pole model now becomes clear: Its use is very general and is not limited to the soft meson limit and to the pseudoscalar-meson final state. Recently, this approach has been applied to the baryonic B decays, e.g., $B \to p\bar{p}$ [15,16]. In this paper we illustrate how to apply the pole model to the decay modes $\Lambda_c^+ \to BP$, BV(V=vector meson). The same technique can be generalized to the nonleptonic decays of bottom baryons.

The main task we have to embark on in the pole model is to evaluate the parity-violating (PV) weak transition elements and strong vertices involving $\frac{1}{2}^-$ baryon intermediate states. We shall employ the wave functions of the MIT bag model. In the bag model the lowest-lying negative-parity baryon states are made of two quarks in the ground $1S_{1/2}$ eigenstate and one quark excited to $1P_{1/2}$ or $1P_{3/2}$. The estimate of strong and weak vertices thus becomes somewhat involved because of the presence of $1P_{1/2}$ and $1P_{3/2}$ bag states.

The layout of this paper is organized as follows. The description of the charmed baryon decay within the framework of the pole model is given in Sec. II. We calculate in Sec. III the branching ratios and the asymmetry parameter α for some selective Cabibbo-allowed two-body nonleptonic decays of Λ_c^+. A comparison of our results with current algebra and other works is made in Sec. IV. Section V contains conclusions and outlook. Details of the general expressions for the baryon-baryon matrix elements and strong coupling constants evaluated in the MIT bag model are presented in Appendixes A–D.

II. POLE MODEL

A. General framework

In general there are three distinct pole contributions (two baryon poles and one meson pole) to baryon weak decays (see Fig. 1 and Ref. [17] for a general discussion). Let us postpone the discussion of the meson-pole contribution for the moment and focus on the baryon intermediate states. We first consider the baryon decay $B_i \to B_f + P$ (P: pseudoscalar meson) and write [18]

$$M(B_i \to B_f + P) = i\bar{u}_f(A + B\gamma_5)u_i \ , \qquad (2.1)$$

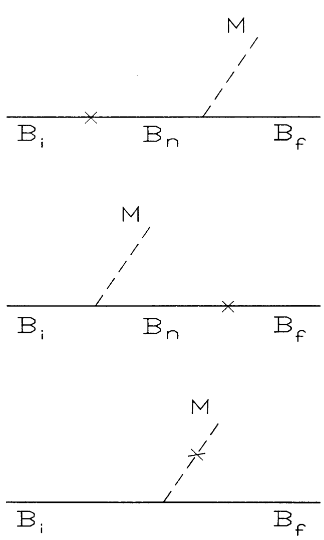

FIG. 1. Pole diagrams for the baryon weak decay $B_i \to B_f + M$.

where A and B are the s- and p-wave decay amplitudes, respectively. It is straightforward to show that the contributions due to the low-lying $B_n(\frac{1}{2}^+)$,$B_n^*(\frac{1}{2}^-)$ and $B_n^*(\frac{1}{2}^+)$ poles are

$$\begin{aligned} A &= \sum_{B_n} \left[\frac{g_{B_f B_n P} b_{ni}}{m_i + m_n} + \frac{b_{fn} g_{B_n B_i P}}{m_f + m_n} \right] - \sum_{B_n^*(1/2^-)} \left[\frac{g_{B_f B_{n^*} P} b_{n^* i}}{m_i - m_{n^*}} + \frac{b_{fn^*} g_{B_{n^*} B_i P}}{m_f - m_{n^*}} \right] , \\ B &= -\sum_{B_n} \left[\frac{g_{B_f B_n P} a_{ni}}{m_i - m_n} + \frac{a_{fn} g_{B_n B_i P}}{m_f - m_n} \right] - \sum_{B_n^*(1/2^+)} \left[\frac{g_{B_f B_{n^*} P} a_{n^* i}}{m_i - m_{n^*}} + \frac{a_{fn^*} g_{B_{n^*} B_i P}}{m_f - m_{n^*}} \right] , \end{aligned} \qquad (2.2)$$

where a_{ij}, a_{i^*j}, and b_{i^*j} are the baryon-baryon matrix elements defined by

$$\begin{aligned} \langle B_i | \mathcal{H}_W | B_i \rangle &= \bar{u}_i (a_{ij} + b_{ij}\gamma_5) u_j \ , \\ \langle B_i^*(\tfrac{1}{2}^-) | \mathcal{H}_W^{\rm PV} | B_j \rangle &= i b_{i^*j} \bar{u}_i u_j \ , \\ \langle B_i^*(\tfrac{1}{2}^+) | \mathcal{H}_W^{\rm PC} | B_j \rangle &= a_{i^*j} \bar{u}_{i^*} \gamma_5 u_j \ . \end{aligned} \qquad (2.3)$$

Note that $b_{ji^*} = -b_{i^*j}$. We did not include in Eq. (2.2) the $B^*(\frac{1}{2}^+)$ pole contribution for s waves and the $B^*(\frac{1}{2}^-)$ term for p waves. It is well known that the PV matrix elements b_{ij} can be disregarded in hyperon nonleptonic decays since they vanish in SU(3) limit. It is also true in charmed baryon decays that $b_{ij} \ll a_{ij}$, as shown explicitly in Refs. [8b,9]. Since $O(b_{i^*j}) = O(a_{ij})$ (see Sec. III) it follows that $b_{ij} \ll b_{i^*j}$ and likewise $a_{i^*j} \ll a_{ij}$. Consequently, the s-wave amplitude of charmed baryon decay is expected to be dominated by the $\frac{1}{2}^-$ baryon states, and the p-wave amplitude by the ground-state $\frac{1}{2}^+$ poles. [This is reinforced by the consideration of the denominator terms in Eq. (2.2).]

As for the decay $B_i \to B_f + V$, its general amplitude is of the form

$$M(B_i \to B_f + V) = i\bar{u}_f(p_f)\epsilon^{*\mu}(A_1\gamma_\mu\gamma_5 + A_2 p_{f\mu}\gamma_5 + B_1\gamma_\mu + B_2 p_{f\mu})u_i(p_i) \ , \qquad (2.4)$$

where ϵ_μ is the polarization vector of the vector meson V. The vector part of the BBV coupling constant leads to

$$\begin{aligned} A_1 &= -\sum_{B_n^*(1/2^-)} \left[\frac{g_{B_f B_{n^*} V} b_{n^* i}}{m_i - m_{n^*}} + \frac{b_{fn^*} g_{B_{n^*} B_i V}}{m_f - m_{n^*}} \right] , \\ B_1 &= -\sum_{B_n} \left[\frac{g_{B_f B_n V} a_{ni}}{m_i - m_n} + \frac{a_{fn} g_{B_n B_i V}}{m_f - m_n} \right] , \\ A_2 &= B_2 = 0 \ , \end{aligned} \qquad (2.5)$$

where only the leading contributions are kept. In principle, a tensor BBV coupling of the form

$$-\frac{1}{4}\frac{f_{B_fB_iV}}{m_V}\bar{B}_f\sigma_{\mu\nu}B_i(\partial^\mu V^\nu-\partial^\nu V^\mu) \tag{2.6}$$

is also allowed. Contributions due to this coupling are

$$A_1=\frac{1}{2m_V}(m_i-m_f)\sum_{B_n^*}\left[\frac{f_{B_fB_n^*V}b_{n^*i}}{m_i-m_{n^*}}+\frac{b_{fn^*}f_{B_{n^*}B_iV}}{m_f-m_{n^*}}\right],$$

$$A_2=2A_1/(m_i-m_f)\ ,\tag{2.7}$$

$$B_1=-\frac{1}{2m_V}(m_i+m_f)\sum_{B_n}\left[\frac{f_{B_fB_nV}a_{ni}}{m_i-m_n}+\frac{a_{fn}f_{B_nB_iV}}{m_f-m_n}\right],$$

$$B_2=-2B_1/(m_i+m_f)\ .$$

Nevertheless, we will neglect the tensor BBV coupling in ensuring calculations.

B. Current algebra

Since current algebra is the most common approach employed before for the study of the nonleptonic weak decay $B_c\to B+P^a$, it is worth examining the relation between this approach and the pole model. For the s-wave amplitude, we write

$$A=A^{\rm CA}+(A-A^{\rm CA})\ ,\tag{2.8}$$

where $A^{\rm CA}=\lim_{q\to 0}A$ is the current-algebra result of A. We keep the term $(A-A^{\rm CA})$ to ensure that A is an on-shell amplitude. Using the usual Goldberger-Treiman (GT) relation for the coupling constants g_{BBP} and the generalized GT relation (D3) for g_{B^*BP} coupling constants, it is not difficult to show that, in the soft meson limit, the s-wave amplitude becomes ($f_\pi=132$ MeV)

$$A^{\rm CA}=\frac{\sqrt{2}}{f_{P^a}}\sum_{B_n}(g_A^{B_fB_n}b_{ni}+b_{fn}g_A^{B_iB_n})-\frac{\sqrt{2}}{f_{P^a}}\sum_{B_n^*(1/2^-)}(g_A^{B_fB_n^*}b_{n^*i}-b_{fn^*}g_A^{B_{n^*}B_i})\ ,\tag{2.9}$$

which is equivalent to the familiar commutator relation

$$A^{\rm CA}=-\frac{\sqrt{2}}{f_{P^a}}\langle B_f|[Q_5^a,\mathcal{H}^{\rm PV}]|B_i\rangle\ .\tag{2.10}$$

In general, the s-wave amplitude is dominated by the $\frac{1}{2}^-$ baryon resonances. The advantage of current algebra is that, when it is appropriate to take the soft pion limit, the parity-violating amplitude is reduced to a simple commutator term, whose evaluation does not require the information of $\frac{1}{2}^-$ poles. It follows from Eqs. (2.2) and (2.9) that

$$A-A^{\rm CA}=-\frac{\sqrt{2}}{f_{P^a}}(m_i-m_f)\left[\frac{g_A^{B_fB_n}b_{ni}}{m_i+m_n}-\frac{b_{fn}g_A^{B_nB_i}}{m_f+m_n}\right]+\frac{\sqrt{2}}{f_{P^a}}(m_i-m_f)\left[\frac{g_A^{B_fB_n^*}b_{n^*i}}{m_i-m_{n^*}}+\frac{b_{fn^*}g_A^{B_{n^*}B_i}}{m_f-m_{n^*}}\right].\tag{2.11}$$

We shall see in Sec. III that the correction term $(A-A^{\rm CA})$, the difference between the pole model and current algebra for the s-wave, is important for charmed baryon decays.

For the p-wave amplitude, we define

$$T_\mu=\int d^4x\, e^{iq\cdot x}\langle B_f|TA_\mu^a(x)\mathcal{H}_W(0)|B_i\rangle\tag{2.12}$$

so that

$$M_{fi}=\left[M_{fi}-i\frac{\sqrt{2}}{f_{P^a}}q_\mu T^\mu\right]+i\frac{\sqrt{2}}{f_{P^a}}q_\mu T^\mu\ .\tag{2.13}$$

It is known that because of the presence of the ground-state baryon poles, neither M_{fi} nor $q_\mu T^\mu$ is defined in the limit $q_\mu\to 0$, but their difference has a well-defined limit [19]. Therefore, the current-algebra expression for the PC amplitude is given by

$$M_{fi}^{\rm CA}=\lim_{q\to 0}\left[M_{fi}-i\frac{\sqrt{2}}{f_{P^a}}q_\mu T^\mu\right]+i\frac{\sqrt{2}}{f_{P^a}}q_\mu T^\mu\ .\tag{2.14}$$

Since the evaluation of $q_\mu T^\mu$ is well known, we simply quote the result [20]

$$B^{\rm CA}=-\frac{\sqrt{2}}{f_{P^a}}\sum_{B_n}\left[g_A^{B_fB_n}\frac{m_f+m_n}{m_i-m_n}a_{ni}+a_{fn}\frac{m_i+m_n}{m_f-m_n}g_A^{B_iB_n}\right].\tag{2.15}$$

The deviation of current algebra from the pole model for p-waves comes from the extrapolation of $(M-i\sqrt{2}/f_Pq_\mu T^\mu)$ from $q^2=0$ to physical q^2.

C. Factorizable contribution

The meson-pole contribution depicted in Fig. 1 is usually identified with the factorizable amplitude. This can be argued based on the fact that the factorization approach empirically works well for meson decays [21] and hence also for meson-meson transition elements. Therefore, meson-pole contributions are dominated by factorizable diagrams. Consider the decay $B_i\to B_f+P$. Its separable contribution is of the form

$$\langle P|A_\mu|0\rangle\langle B_f|V^\mu+A^\mu|B_i\rangle\ .\tag{2.16}$$

The vector and axial-vector form factors of

$\langle B_f|V_\mu+A_\mu|B_i\rangle$ are dominated by the low-lying 1^+ and 1^- meson states, respectively. For example, $K^*(892)$ and $K_1(1270)$ poles give rise to the factorizable s- and p-wave amplitudes, respectively, for hyperon decay. Likewise, there are $D_s(D)$ and $D_s^*(D^*)$ meson-pole contributions to charmed baryon decays. Because of the lack of experimental information on the weak matrix elements $\langle\pi|\mathcal{H}_W|D^*\rangle$, etc., we shall rely on the factorization approach.

To proceed, we shall consider the QCD-corrected effective weak Hamiltonian for the Cabibbo-allowed charmed baryon decay:

$$\mathcal{H}_W=\frac{G_F}{2\sqrt{2}}\cos^2\theta_C(c_-O_-+c_+O_+) \tag{2.17}$$

with $O_\pm=(\bar{s}c)(\bar{u}d)\pm(\bar{s}d)(\bar{u}c)$, where $(\bar{q}_1q_2)=\bar{q}_1\gamma_\mu(1+\gamma_5)q_2$, and θ_C is the Cabibbo mixing angle. The Wilson coefficients are evaluated at the charm mass scale to be $c_+\cong0.73$ and $c_-\cong1.90$. For $\Lambda_c^+\to B_f+P$ decay, the factorizable amplitudes are given by $(k=1,2)$

$$A^{\rm fac}=-\frac{1}{\sqrt{2}}G_F\cos^2\theta_C f_P c_k(m_{\Lambda_c^+}-m_f)f_1^{\Lambda_c^+B_f}(m_P^2)\,, \tag{2.18}$$

$$B^{\rm fac}=\frac{1}{\sqrt{2}}G_F\cos^2\theta_C f_P c_k(m_{\Lambda_c^+}+m_f)g_1^{\Lambda_c^+B_f}(m_P^2)\,,$$

where f_P is the decay constant of the meson P, c_1 (c_2) is for π^+ $(\bar{K}^0)$ emission, and f_1 as well as g_1 are the form factors defined by

$$\langle B_f(p_f)|V_\mu+A_\mu|B_i(p_i)\rangle =\bar{u}_f(p_f)\left[f_1\gamma_\mu-\frac{f_2}{m_i}i\sigma_{\mu\nu}q^\nu+\frac{f_3}{m_i}q_\mu +g_1\gamma_\mu\gamma_5-\frac{g_2}{m_i}i\sigma_{\mu\nu}q^\nu\gamma_5 +\frac{g_3}{m_i}q_\mu\gamma_5\right]u_i(p_i)\,, \tag{2.19}$$

with $q_\mu=(p_i-p_f)_\mu$. In the conventional vacuum-insertion method, $c_1=(2c_++c_-)/3$ and $c_2=(2c_+-c_-)/3$. However, we have learned from the nonleptonic decays of charmed and bottom mesons that the naive vacuum-saturation approximation, in which the Fierz-transformed terms are taken into consideration, fails to account for the bulk of data, especially for those decay modes which are naively expected to be color suppressed (see Ref. [21] for a review). The discrepancy between theory and experiment is greatly improved in the large N_c version of the factorization approach [22]. It amounts to dropping the Fierz-transformed contributions. Hence,

$$c_1=\tfrac{1}{2}(c_++c_-)\,,\quad c_2=\tfrac{1}{2}(c_+-c_-)\,. \tag{2.20}$$

Note that $(c_+-c_-)/2\simeq-0.59$ and $(2c_+-c_-)/3\simeq-0.15$. This means that the decay modes, e.g., $\Lambda_c^+\to p\bar{K}^0$, $p\phi$ are color and QCD-correction suppressed according to the usual vacuum-insertion method, but not so in the $1/N_c$ approach. We shall see later that the experimental observation of $\Lambda_c^+\to p\phi$ and the ratio of $\Gamma(p\bar{K}^0)/\Gamma(\Lambda\pi^+)$ strongly support the latter expectation. Before proceeding, it is worth clarifying a point here. The value of c_2 is chosen in Refs. [11,12] to be in the range of 0.4 to 0.7 with a sign opposite to ours. This sign difference will affect the predicted decay rate of $\Lambda_c^+\to p\bar{K}^0, p\bar{K}^{*0}$, as we shall discuss in Sec. IV.

For the decay $\Lambda_c^+\to B_f+V$, it is easily shown that $(k=1,2)$

$$\begin{aligned}
A_1^{\rm fac}&=-\frac{G_F}{\sqrt{2}}\cos^2\theta_C c_k f_V m_V\left[g_1^{\Lambda_c^+B_f}(m_V^2)-g_2^{\Lambda_c^+B_f}(m_V^2)\frac{m_{\Lambda_c^+}-m_f}{m_{\Lambda_c^+}}\right],\\
A_2^{\rm fac}&=\frac{G_F}{\sqrt{2}}\cos^2\theta_C c_k f_V m_V[2g_2^{\Lambda_c^+B_f}(m_V^2)/m_{\Lambda_c^+}]\,,\\
B_1^{\rm fac}&=-\frac{G_F}{\sqrt{2}}\cos^2\theta_C c_k f_V m_V\left[f_1^{\Lambda_c^+B_f}(m_V^2)+f_2^{\Lambda_c^+B_f}(m_V^2)\frac{m_{\Lambda_c^+}+m_f}{m_{\Lambda_c^+}}\right],\\
B_2^{\rm fac}&=\frac{G_F}{\sqrt{2}}\cos^2\theta_C c_k f_V m_V[2f_2^{\Lambda_c^+B_f}(m_V^2)/m_{\Lambda_c^+}]\,,
\end{aligned} \tag{2.21}$$

where form factors are evaluated at $q^2=m_V^2$, f_V is defined by

$$\langle V|(\bar{q}_1q_2)|0\rangle=-if_Vm_V\epsilon_\mu^*\,, \tag{2.22}$$

and c_1 (c_2) is for ρ^+ $(\bar{K}^{*0})$ emission.

D. Kinematics

Two quantities of experimental interest are the partial decay rate and the asymmetry parameter α. We quote in this subsection the basic formulas needed for calculation. For the decay $B_i\to B_f+P$, the unpolarized decay rate is given by

$$\Gamma=\frac{p_c}{8\pi}\left[\frac{(m_i+m_f)^2-m_P^2}{m_i^2}|A|^2+\frac{(m_i-m_f)^2-m_P^2}{m_i^2}|B|^2\right] \tag{2.23}$$

with p_c being the c.m. three-momentum in the rest frame of B_i, and the up-down asymmetry α reads

$$\alpha=\frac{2\kappa\,{\rm Re}(A^*B)}{|A|^2+\kappa^2|B|^2} \tag{2.24}$$

with $\kappa=p_c/(E_f+m_f)$.

The kinematics of $B_i\to B_f+V$ has been analyzed in detail in Ref. [11] (see also Ref. [2]). The total decay rate in the unpolarized case is given by

$$\Gamma=\frac{1}{8\pi}\frac{E_V+m_V}{E_i}p_c\left[2(|S|^2+|P_2|^2)+\frac{E_V^2}{m_V^2}(|S+D|^2+|P_1|^2)\right], \quad (2.25)$$

with

$$P_1=-\frac{p_c}{E_V}\left[\frac{m_i+m_f}{E_f+m_f}B_1+m_iB_2\right],$$
$$P_2=\frac{p_c}{E_f+m_f}B_1, \quad (2.26)$$
$$S=A_1, \quad D=-\frac{p_c^2}{E_V(E_f+m_f)}(A_1-A_2m_i),$$

where E_V and E_f are the energies of the vector meson and the daughter baryon, respectively. Note that we have neglected the contributions due to the tensor BBV coupling. The up-down asymmetry is [11]

$$\alpha=\frac{4m_V^2\mathrm{Re}(S^*P_2)+2E_V^2\mathrm{Re}(S+D)^*P_1}{2(|S|^2+|P_2|^2)m_V^2+(|S+D|^2+|P_1|^2)E_V^2}. \quad (2.27)$$

III. NONLEPTONIC WEAK DECAYS OF CHARMED BARYONS

The general expression for the two-body nonleptonic decay of charmed baryons consists of three ingredients: the PC (PV) baryon matrix elements a_{ij} (b_{i^*j}), the coupling constants g_{BBP}, g_{BBV}, and the form factors f_i and g_i. In the following we will discuss the evaluation of these ingredients in order. For definiteness, we choose in this paper the decay channels: $\Lambda_c^+\to\Lambda\pi^+(\rho^+)$, $p\bar{K}^0(\bar{K}^{*0})$, $\Sigma^+\pi^0(\rho^0)$, $\Sigma^0\pi^+(\rho^+)$.

A. Baron-baryon matrix elements

The evaluation of the PC baryon matrix elements a_{ij} and PV ones b_{i^*j} within the MIT bag model is presented in detail in Appendixes B and C. For numerical estimates we use the bag parameters

$$m_u=m_d=0, \quad m_s=0.279 \text{ GeV}, \quad m_c=1.551 \text{ GeV},$$
$$x_u=2.043, \quad x_s=2.488, \quad x_c=2.948, \quad R=5 \text{ GeV}^{-1} \quad (3.1)$$

for $nL_J=1S_{1/2}$ quarks [23],

$$x_u=3.81, \quad x_s=3.96, \quad R=5.3 \text{ GeV}^{-1} \quad (3.2)$$

for $1P_{1/2}$ quarks, and

$$x_u=3.20, \quad x_s=3.65, \quad R=5.2 \text{ GeV}^{-1} \quad (3.3)$$

for $1P_{3/2}$ quarks. The eigenvalue x_q is determined by the transcendental equation Eq. (A5).

Since the four-quark operator O_+ is symmetric in color indices, it does not contribute to the baryon-baryon matrix element. In Eq. (B4) the PC O_--induced $\frac{1}{2}^+-\frac{1}{2}^+$ weak transitions are expressed in terms of two four-quark overlap bag integrals X_1 and X_2, defined in Eq. (B3). Using the bag wave function given in Appendix A, we find numerically

$$X_1=-3.58\times10^{-6} \text{ GeV}^3, \quad X_2=1.74\times10^{-4} \text{ GeV}^3. \quad (3.4)$$

For later convenience, we will factor out the common factor $G_F\cos^2\theta_C$ in Eq. (2.3), so the new baryon matrix elements become

$$a_{ij}=\frac{c_-}{2\sqrt{2}}\langle B_i|O_-^{\mathrm{PC}}|B_j\rangle,$$
$$b_{i^*j}=-i\frac{c_-}{2\sqrt{2}}\langle B_i(1/2^-)|O_-^{\mathrm{PV}}|B_j\rangle. \quad (3.5)$$

The factor of $G_F\cos^2\theta_C$ will be put back when necessary. It follows from Eqs. (B4) and (3.4) that (in terms of c_- GeV^3) [24]

$$a_{\Sigma^+\Lambda_c^+}=a_{\Sigma_c^0\Lambda^0}=-3.76\times10^{-3},$$
$$a_{\Sigma_c^+\Sigma^+}=a_{\Sigma_c^0\Sigma^0}=6.58\times10^{-3}. \quad (3.6)$$

The evaluation of the $\frac{1}{2}^--\frac{1}{2}^+$ baryon matrix elements b_{i^*j} is much more involved. This is because the physical $\frac{1}{2}^-$ baryon states are linear combinations of $(S_{1/2})^2P_{1/2}$ and $(S_{1/2})^2P_{3/2}$ quark eigenstates. Consequently, the number of the relevant bag overlap integrals [Eqs. (C9) and (C15)] is largely increased. Assuming that the $\frac{1}{2}^-$ pole contributions are dominated by the low-lying negative parity (70, $L=1$) states, we obtain (in units of GeV^3)

$$\tilde{X}_1=2.433\times10^{-5}, \quad \tilde{X}_2=1.771\times10^{-4}, \quad \underset{\sim}{X}_1=1.350\times10^{-4},$$
$$\tilde{X}_1'=9.651\times10^{-6}, \quad \tilde{X}_2'=1.624\times10^{-4}, \quad \underset{\sim}{X}_1'=4.077\times10^{-5}, \quad (3.7)$$
$$\tilde{X}_{1s}=2.782\times10^{-5}, \quad \tilde{X}_{2s}=1.427\times10^{-4}, \quad \underset{\sim}{X}_{1s}=1.423\times10^{-4}.$$

It follows from Eqs. (A7), (C8), (C14)–(C19) and (3.7) that (in units of c_- GeV^3)

$$b_{\Sigma^+(^28)\Lambda_c^+}=-1.76\times10^{-3}, \quad b_{\Sigma^+(^48)\Lambda_c^+}=-4.21\times10^{-3}, \quad b_{\Sigma^+(^210)\Lambda_c^+}=1.47\times10^{-4},$$
$$b_{\Sigma_c^0(^28)\Lambda^0}=1.56\times10^{-3}, \quad b_{\Sigma_c^0(^48)\Lambda^0}=1.72\times10^{-3}, \quad b_{\Sigma^+(^210)\Lambda^0}=-7.97\times10^{-4},$$
$$b_{\Sigma_c^0(^28)\Sigma^0}=-2.95\times10^{-3}, \quad b_{\Sigma_c^0(^48)\Sigma^0}=-2.86\times10^{-3}, \quad b_{\Sigma_c^0(^210)\Sigma^0}=1.46\times10^{-3}, \quad (3.8)$$
$$b_{\Sigma_c^+(^28)\Sigma^+}=2.95\times10^{-3}, \quad b_{\Sigma_c^+(^48)\Sigma^+}=2.86\times10^{-3}, \quad b_{\Sigma_c^+(^210)\Sigma^+}=-1.46\times10^{-3},$$

where $\Sigma^+(^28)$ is the short-hand notation for $\Sigma^+(70,\frac{1}{2}^-,{}^28_{1/2})$, etc. It should be stressed again that attention should be paid to the indices of the $\frac{1}{2}^- - \frac{1}{2}^+$ matrix element as $b_{i^*j} = -b_{ji^*}$.

B. Coupling constants

The strong coupling constants g_{BBP} and g_{BBV} are given by Eqs. (D1) and (D2), respectively. As for the couplings g_{B^*BP} and g_{B^*BV}, the former is related to the axial-vector coupling $g^a_{B^*B}$ via the generalized Goldberger-Treiman relation Eq. (D3), while the latter can be connected to g_{BBV} through Eq. (D8). Since $\langle B^*(P_{3/2})|b^\dagger_{\tilde q} b_q(\sigma_z \hat{\mathbf{r}}_z)|B(S_{1/2})\rangle = 0$, it is clear from Eq. (D4) that $g^A_{B^*B}$ is determined by the matrix element $\int d\Omega \langle B^*|b^\dagger_{\tilde q} b_q|B\rangle$ (see Appendix A for the notation $\tilde q$ and $\underset{\sim}{q}$) and the overlap integrals $\tilde Y_1$ and $\tilde Y_{1s}$ [Eq. (D13)], whose values are

$$\tilde Y_1 = 0.056 \ , \quad \tilde Y_{1s} = 0.051 \ . \tag{3.9}$$

We quote our final results for g_{B^*BP}:

$$\begin{aligned}
&g_{\Sigma^+(^28)p\bar K^0} = 0.52 \ , \quad g_{\Sigma^+(^48)p\bar K^0} = 2.49 \ , \quad g_{\Sigma^+(^210)p\bar K^0} = 0.81 \ , \\
&g_{\Sigma^+(^28)\Lambda^0\pi^+} = -0.63 \ , \quad g_{\Sigma^+(^48)\Lambda^0\pi^+} = 1.59 \ , \quad g_{\Sigma^+(^210)\Lambda^0\pi^+} = -1.11 \ , \\
&g_{\Sigma^+(^28)\Sigma^0\pi^+} = 1.55 \ , \quad g_{\Sigma^+(^48)\Sigma^0\pi^+} = 0.81 \ , \quad g_{\Sigma^+(^210)\Sigma^0\pi^0} = -0.59 \ , \\
&g_{\Sigma_c^0(^28)\Lambda_c^+\pi^+} = -0.72 \ , \quad g_{\Sigma_c^0(^48)\Lambda_c^+\pi^+} = 1.43 \ , \quad g_{\Sigma_c^0(^210)\Lambda_c^+\pi^+} = -0.72 \ ,
\end{aligned} \tag{3.10}$$

where uses have been made of Eq. (A.7), $m_{\Sigma_c^*} \sim 2.75$ GeV, and [25]

$$m_{\Sigma(^28)} = 1620 \text{ MeV} \ , \quad m_{\Sigma(^48)} = 1750 \text{ MeV} \ , \quad m_{\Sigma(^210)} \simeq 2 \text{ GeV} \ . \tag{3.11}$$

It is worth noting that although $g^A_{BB^*} = -g^A_{B^*B}$, the coupling constant g_{BB^*P} (also g_{BB^*V}) is the same as g_{B^*BP}.

To compute g_{B^*BV}, we need to evaluate the matrix elements $\int d\Omega \langle B^*|b^\dagger_{\tilde q} b_q \sigma_z|B\rangle$ and $\int d\Omega \langle B^*|b^\dagger_{\underset{\sim}{q}} b_q \hat{\mathbf{r}}_z|B\rangle$ [see Eq. (D8)]. The numerical results are

$$\begin{aligned}
&g_{\Sigma^+(^28)p\bar K^{*0}} = -5.41\times10^{-3} g_{\Sigma^+p\bar K^{*0}} \ , \quad g_{\Sigma^+(^48)p\bar K^{*0}} = 3.49\times10^{-2} g_{\Sigma^+p\bar K^{*0}} \ , \\
&g_{\Sigma^+(^210)p\bar K^{*0}} = -5.41\times10^{-3} g_{\Sigma^+p\bar K^{*0}} \ , \quad g_{\Sigma^+(^28)\Lambda\rho^+} = 9.06\times10^{-2} g_{\Sigma^+\Lambda\rho^+} \ , \\
&g_{\Sigma^+(^48)\Lambda\rho^+} = 3.77\times10^{-2} g_{\Sigma^+\Lambda\rho^+} \ , \quad g_{\Sigma^+(^210)\Lambda\rho^+} = -1.53\times10^{-2} g_{\Sigma^+\Lambda\rho^+} \ , \\
&g_{\Sigma^+(^28)\Sigma^0\rho^+} = -1.39\times10^{-1} g_{\Sigma^+\Sigma^0\rho^+} \ , \quad g_{\Sigma^+(^48)\Sigma^0\rho^+} = 2.18\times10^{-2} g_{\Sigma^+\Sigma^0\rho^+} \ , \\
&g_{\Sigma^+(^210)\Sigma^0\rho^+} = -8.80\times10^{-3} g_{\Sigma^+\Sigma^0\rho^+} \ , \quad g_{\Sigma_c^0(^28)\Lambda_c^+\rho^+} = -1.12\times10^{-1} g_{\Sigma_c^0\Lambda_c^+\rho^+} \ , \\
&g_{\Sigma_c^0(^48)\Lambda_c^+\rho^+} = -4.66\times10^{-2} g_{\Sigma_c^0\Lambda_c^+\rho^+} \ , \quad g_{\Sigma_c^0(^210)\Lambda_c^+\rho^+} = 1.87\times10^{-2} g_{\Sigma_c^0\Lambda_c^+\rho^+} \ ,
\end{aligned} \tag{3.12}$$

where we have used the bag integrals [Eq. (D9)]

$$\begin{aligned}
&\tilde Y_2 = 1.87\times10^{-2} \ , \quad \tilde Y_{2s} = 8.86\times10^{-3} \ , \\
&\underset{\sim}{Y}_1 = 4.31\times10^{-3} \ , \quad \underset{\sim}{Y}_{1s} = 2.07\times10^{-2} \ .
\end{aligned} \tag{3.13}$$

Assuming universality for the vector BBV coupling, namely, $g_{K^*} = g_\rho = g$, it is clear from Eqs. (D2)–(D4) and (D8) that all BBV and hence B^*BV coupling constants appearing in the pole amplitudes can be expressed in terms of $g_{pn\rho^+} = g/\sqrt{2} = 5.583$ extracted from experiment.

C. Form factors

Contrary to the conventional quark- or bag-model calculation of the form factors at $q^2=0$, the form factors f_i and g_i defined in Eq. (2.19) are evaluated by Pérez-Marcial *et al.* [26] in the Breit frame where $\mathbf{p}_i = -\mathbf{p}_f = \mathbf{q}/2$. Furthermore, they choose $\mathbf{q}=0$ so that both baryons are *static* in the Breit frame and thus the static-bag and quark-model wave functions best resemble the compound hadron states. Note that in this frame the four-momentum transfer squared is maximum; that is, $q^2 = (m_i - m_f)^2$. In fact, based on the heavy quark symmetry one can make first-principles predictions for the form factors which appear in heavy hadron-hadron transitions in the limit of maximum q^2 [27].

Once the form factors at $q^2 = (m_i - m_f)^2$ are evaluated using the quark or bag model, their values at $q^2=0$ can be obtained by assuming a monopole or dipole q^2 dependence of the form factors

$$f_i(q^2) = \frac{f_i(0)}{(1-q^2/m_*^2)^n} \ , \quad g_i(q^2) = \frac{g_i(0)}{(1-q^2/m_A^2)^n} \ , \tag{3.14}$$

with $n=1$ or 2. The evaluation of $f_i(q^2)$ and $g_i(q^2)$ in the MIT bag mode was already done in Ref. [26]. The results relevant for our purposes are

$$f_1^{\Lambda_c^+\Lambda}(0)=0.46\ ,\quad f_2^{\Lambda_c^+\Lambda}(0)=0.19\ ,$$
$$g_1^{\Lambda_c^+\Lambda}(0)=0.50\ ,\quad g_2^{\Lambda_c^+\Lambda}(0)=-0.05\ , \tag{3.15}$$

for $n=2, m_*=2.11$ GeV, $m_A=2.54$ GeV [25]. With these values of form factors, the branching ratio of the exclusive $\Lambda_c^+\to\Lambda$ decay is predicted by the MIT bag model to be 1.5% (see Table VIII of Ref. [26]; corrections due to the updated Λ_c^+ lifetime have been made), which is in good agreement with the recent ARGUS measurements [29] $B(\Lambda_c^+\to\Lambda e^+X)=(1.6\pm0.7)\%$ and $B(\Lambda_c^+\to\Lambda\mu^+X)=(1.5\pm0.9)\%$.

To compute the factorizable amplitude of $\Lambda_c^+\to p\bar{K}^0(\bar{K}^{*0})$, one will encounter the matrix element $\langle p|J_\mu|\Lambda_c^+\rangle$, whose form factors are related to that of $\Lambda_c^+\to\Lambda$ by the SU(3) relation

$$f_i^{\Lambda_c^+p}(0)=-(\tfrac{3}{2})^{1/2}f_i^{\Lambda_c^+\Lambda}(0)\ ,$$
$$g_i^{\Lambda_c^+p}(0)=-(\tfrac{3}{2})^{1/2}g_i^{\Lambda_c^+\Lambda}(0)\ , \tag{3.16}$$

for $m_*=2.01$ GeV and $m_A=2.42$ GeV [25]. The minus sign appearing in Eq. (3.16) is due to the negative relative sign between the wave function of Λ_c^+ and p [cf. Eq. (A10)].

D. Color nonsuppression

Before proceeding to compute the decay rates of the Cabibbo-favored decay of Λ_c^+, we first pay attention to the Cabibbo-suppressed mode $\Lambda_c^+\to p\phi$. This decay is of particular interest because it receives contributions only from the factorizable diagram and because it is naively expected to be color suppressed in the conventional vacuum-insertion approach. The calculation is very straightforward. From Eqs. (3.14)–(3.16), (2.26), and (2.21) with $\cos^2\theta_C$ replaced by $\sin\theta_C\cos\theta_C$ we obtain ($h'\equiv G_F\sin\theta_C\cos\theta_C$)

$$S=-0.106h'\ ,\quad P_1=8.39\times10^{-2}h'\ ,$$
$$P_2=-4.59\times10^{-2}h'\ ,\quad D=1.27\times10^{-2}h'\ , \tag{3.17}$$

where uses of $f_\phi=230$ MeV extracted from the measured $\phi\to e^+e^-$ rate and the $1/N_c$ relation $c_2=(c_+-c_-)/2$ have been made. It follows from Eq. (2.25) that

$$B(\Lambda_c^+\to p\phi)=1.95\times10^{-3}\ , \tag{3.18}$$

where we have used $\Gamma(\Lambda_c^+\to\text{all})=3.45\times10^{-12}$ GeV [25]. Experimentally, this channel has been measured by the Amsterdam-Bristol-CERN-Cracow-Munich-Rutherford (ACCMOR) Collaboration (CERN NA32 experiment) with the result $B(\Lambda_c^+\to p\phi)=(0.04\pm0.027)B(\Lambda_c^+\to pK^-\pi^+)$ [30]. Using the current value [31] of $B(\Lambda_c^+\to pK^-\pi^+)=(4.3\pm1.1)\%$, it is evident that theory is in good agreement with the central value of the measured branching ratio.

There are two important consequences we can learn from this exercise. First, color suppression is not operative (at least for the factorizable diagrams). If c_2 were equal to $(2c_+-c_-)/3$ as advocated in the vacuum-insertion approach, the decay rate of $\Lambda_c^+\to p\phi$ would have turned out to be too small by a factor of 15, in violent disagreement with data. Second, apart from the MIT bag model, form factors and baryon-baryon matrix elements have also been evaluated in the so-called heavy quark bag model in which the single heavy quark occupies the center of the bag and light quarks move around it [32]. The heavy-quark bag model tends to give smaller values for form factors, coupling constants and weak transition elements [8c]. Obviously, the experimental measurement of $\Lambda_c^+\to p\phi$ favors the MIT bag model's results of f_i and g_i for $\Lambda_c^+\to p$ transition.

E. Branching ratios

Having all the necessary ingredients evaluated in Secs. III A–III C, we are ready to compute the branching ratios and the α asymmetry parameter for the two-body nonleptonic weak decays of Λ_c^+. The results are exhibited in Tables I and II. To illustrate the calculation, we consider the decay modes $\Lambda_c^+\to p\bar{K}^0, \Sigma^0\pi^+$, and $\Lambda\rho^+$.

$\Lambda_c^+\to p\bar{K}^0$. The factorizable amplitudes obtained from Eqs. (2.18), (2.20), and (3.16) are

$$A^{\text{fac}}=-5.73\times10^{-2}h\ ,\quad B^{\text{fac}}=0.143h\ , \tag{3.19}$$

with $h\equiv G_F\cos^2\theta_C$. Note that A and B are dimensionless, and G_F is in units of GeV^{-2}. The pole amplitudes are given by

$$A^{\text{pole}}\simeq-\left[\frac{g_{\Sigma^+(^28)p\bar{K}^0}b_{\Sigma^+(^28)\Lambda_c^+}}{m_{\Lambda_c^+}-m_{\Sigma^+(^28)}}+\frac{g_{\Sigma^+(^48)p\bar{K}^0}b_{\Sigma^+(^48)\Lambda_c^+}}{m_{\Lambda_c^+}-m_{\Sigma^+(^48)}}+\frac{g_{\Sigma^+(^210)p\bar{K}^0}b_{\Sigma^+(^210)\Lambda_c^+}}{m_{\Lambda_c^+}-m_{\Sigma^+(^210)}}\right]$$
$$=3.91\times10^{-2}h\ , \tag{3.20}$$

TABLE I. Numerical values of the predicted s- and p-wave amplitudes of $\Lambda_c^+\to B+P$ decays in units of $G_F\cos^2\theta_C\times10^{-2}$ GeV^2. The theoretical and experimental branching ratios (in percent) and the predicted α asymmetry parameter are given in the last three columns. The lifetime of the charmed baryon Λ_c^+ is taken to be 1.91×10^{-13} s (Ref. [25]).

Reaction	A^{fac}	A^{pole}	A^{tot}	B^{fac}	B^{pole}	B^{tot}	α	(BR)$_{\text{theory}}$	(BR)$_{\text{expt}}$
$\Lambda_c^+\to p\bar{K}^0$	−5.73	3.91	−1.82	14.33	3.23	17.56	−0.49	1.2	2.1±0.6
$\Lambda_c^+\to\Lambda\pi^+$	−5.40	1.95	−3.45	18.09	−4.87	13.22	−0.96	0.87	0.8±0.3
$\Lambda_c^+\to\Sigma^0\pi^+$	0	2.44	2.44	0	14.63	14.63	0.83	0.72	0.80±0.35
$\Lambda_c^+\to\Sigma^+\pi^0$	0	−2.44	−2.44	0	−14.63	−14.63	0.83	0.72	

TABLE II. Same as Table I except for $\Lambda_c^+ \to B + V$ decays. The upper (lower) entry is for $\beta=0(\frac{3}{4})$.

Reaction	$A_1^{\rm fac}$	$A_1^{\rm pole}$	$A_2^{\rm fac}$	$A_2^{\rm pole}$	$B_1^{\rm fac}$	$B_1^{\rm pole}$	$B_2^{\rm fac}$	$B_2^{\rm pole}$	α	$({\rm BR})_{\rm theory}$
$\Lambda_c^+ \to p\bar{K}^{*0}$	-7.12	-0.28	-0.58	0	-11.32	-3.64	2.58	0	-0.15	3.3
	-7.12	0.14	-0.58	0	-11.32	1.82	2.58	0	-0.05	1.8
$\Lambda_c^+ \to \Lambda\rho^+$	-8.64	0	-0.71	0	-13.33	0	2.99	0	-0.19	2.6
	-8.64	0.36	-0.71	0	-13.33	0.40	2.99	0	-0.19	2.3
$\Lambda_c^+ \to \Sigma^0\rho^+$	0	0.29	0	0	0	-5.15	0	0	0.06	0.19
	0	-0.13	0	0	0	2.11	0	0	0.07	0.03
$\Lambda_c^+ \to \Sigma^+\rho^0$	0	-0.29	0	0	0	5.15	0	0	0.06	0.19
	0	0.13	0	0	0	-2.11	0	0	0.07	0.03

and

$$B^{\rm pole} = -\frac{g_{\Sigma^+ p\bar{K}^0} a_{\Lambda_c^+\Sigma^+}}{m_{\Lambda_c^+} - m_{\Sigma^+}} = 3.23\times 10^{-2}h \ , \qquad (3.21)$$

where we have applied the results of Secs. III A and III B. Therefore, the total s- and p-wave amplitudes turn out to be

$$A^{\rm tot} = -1.82\times 10^{-2}h \ , \quad B^{\rm tot} = 0.176h \ . \qquad (3.22)$$

Consequently,

$$B(\Lambda_c^+ \to p\bar{K}^0) = 1.2\% \ , \quad \alpha = 0.49 \ , \qquad (3.23)$$

to be compared with the experimental value $B(\Lambda_c^+ \to p\bar{K}^0) = (2.1\pm 0.6)\%$ [31].

$\Lambda_c^+ \to \Sigma^0\pi^+$. This decay does not receive factorizable contributions and hence provides a measure of the nonspectator diagrams. The pole amplitudes are

$$A^{\rm pole} = -\sum_{\Sigma^{*+}(1/2^-)} \frac{g_{\Sigma^0\Sigma^{*+}\pi^+} b_{\Sigma^{*+}\Lambda_c^+}}{m_{\Lambda_c^+} - m_{\Sigma^{*+}}} - \sum_{\Sigma_c^{*0}(1/2^-)} \frac{b_{\Sigma^0\Sigma_c^{*0}} g_{\Sigma_c^{*0}\Lambda_c^+\pi^+}}{m_{\Sigma^0} - m_{\Sigma_c^{*0}}} = 2.44\times 10^{-2}h \ ,$$

$$B^{\rm pole} = -\left[\frac{g_{\Sigma^0\Sigma^+\pi^+} a_{\Sigma^+\Lambda_c^+}}{m_{\Lambda_c^+} - m_{\Sigma^+}} + \frac{a_{\Sigma^0\Sigma_c^0} g_{\Sigma_c^0\Lambda_c^+\pi^+}}{m_{\Sigma^0} - m_{\Sigma_c^0}}\right] = 0.146h \ , \qquad (3.24)$$

which lead to

$$B(\Lambda_c^+ \to \Sigma^0\pi^+) = 0.72\% \ , \quad \alpha = 0.83 \ . \qquad (3.25)$$

A very recent CLEO experiment [33] measures $B(\Lambda_c^+ \to \Sigma^0\pi^+) = (1.0\pm 0.2\pm 0.1)B(\Lambda_c^+ \to \Lambda\pi^+)$, which is equal to $(0.80\pm 0.35)\%$ with $B(\Lambda_c^+ \to \Lambda\pi^+) = (0.8\pm 0.3)\%$ [31].

Note that the decay amplitude of $\Lambda_c^+ \to \Sigma^0\pi^+(\rho^+)$ is the same as $\Lambda_c^+ \to \Sigma^+\pi^0(\rho^0)$ except for an overall sign difference.

$\Lambda_c^+ \to \Lambda\rho^+$. Using $f_\rho = f_{K^*} = 0.221$ GeV and Eqs. (2.21) and (3.15) we get

$$A_1^{\rm fac} = -8.64\times 10^{-2}h \ , \quad A_2^{\rm fac} = -7.08\times 10^{-3}h \ ,$$
$$B_1^{\rm fac} = -0.133h \ , \quad B_2^{\rm fac} = 2.99\times 10^{-2}h \ . \qquad (3.26)$$

As for the pole diagrams, we find

$$A_1^{\rm pole} = -\sum_{\Sigma^{*+}} \frac{g_{\Sigma^+\Lambda\rho^+} b_{\Sigma^{*+}\Lambda_c^+}}{m_{\Lambda_c^+} - m_{\Sigma^{*+}}} - \sum_{\Sigma_c^{*0}} \frac{b_{\Lambda\Sigma_c^{*0}} g_{\Lambda_c^+\Sigma_c^{*0}\rho^+}}{m_\Lambda - m_{\Sigma_c^{*0}}} = \begin{cases} 0 \ \text{ for } \beta=0 \ , \\ 3.63\times 10^{-3}h \ \text{ for } \beta=\frac{3}{4} \ , \end{cases} \qquad (3.27)$$

and

$$B_1^{\rm pole} = -\left[\frac{g_{\Sigma^+\Lambda\rho^+} a_{\Sigma^+\Lambda_c^+}}{m_{\Lambda_c^+} - m_{\Sigma^*}} + \frac{a_{\Lambda\Sigma_c^0} g_{\Lambda_c^+\Sigma_c^0\rho^+}}{m_\Lambda - m_{\Sigma_c^0}}\right] = \begin{cases} 0 \ , \ \text{ for } \beta=0 \ , \\ 4.02\times 10^{-3}h \ , \ \text{ for } \beta=\frac{3}{4} \ , \end{cases} \qquad (3.28)$$

where the parameter β measures the mixing of the F- and D-type couplings (see Appendix D). The branching ratio and the α asymmetry parameter are predicted to be

$$B(\Lambda_c^+ \to \Lambda\rho^+) = \begin{cases} 2.560004, \ \alpha = -0.193, \ \text{ for } \beta=0 \ , \\ 2.330004, \ \alpha = -0.189, \ \text{ for } \beta=\frac{3}{4} \ . \end{cases} \qquad (3.29)$$

It is clear from Tables I and II that the pole-model predictions are in good agreement with experiment. We also see that the nonspectator (pole) contributions are usually smaller than the factorizable ones for the decay modes which receive contributions from the factorizable diagram. This is particularly true for $\Lambda_c^+ \to B + V$.

IV. DISCUSSION

A. Comparison with current algebra

Since the decay $B_c \to B + P$ is traditionally studied by the method of current algebra, it is pertinent to compare our pole-model results with the former approach. The predicted branching ratios based on current algebra are summarized in Table III. We see that current algebra

TABLE III. Comparison between various theoretical calculations and experiments for the branching ratios (in percent) of $\Lambda_c^+ \to B + P$ decays. Calculations of Ref. [13] are done in (a) MIT bag model, (b) heavy-quark bag model with MIT-bag parameters, and (c) heavy-quark bag model with heavy-quark bag parameters. The lifetime of the charmed baryon Λ_c^+ is taken to be 1.91 $\times 10^{-13}$ s (Ref. [25]).

	$\Lambda_c^+ \to p\bar{K}^0$	$\Lambda_c^+ \to \Lambda\pi^+$	$\Lambda_c^+ \to \Sigma^0\pi^+$	$\Lambda_c^+ \to \Sigma^+\pi^0$
Guberina *et al.* [6]	2.2	14		
Hussain and Scadron [7] Hussain and Khan [7]	0.7	1.5	4.2	4.2
Ebert and Kallies				
(a) MIT bag [8a,8b]	3.2	7.2	2.3	
(b) heavy-quark bag [8c]	0.3	0.6	0.4	
Cheng [9]	1.8	6.8	1.9	
Kalinovsky *et al.* [10]				
(a) without $1^{\pm}$ meson poles	5.7	3.4	0.03	0.03
(b) with $1^{\pm}$ meson poles	4.0	1.9	8×10^{-3}	8×10^{-3}
Pakvasa *et al.* [11]	5.3	1.9		
Kaur and Khanna [12]				
(a) symmetric couplings	7.6	1.9	11.2	
(b) broken couplings	8.6	2.8	11.2	
Turan and Eeg [13]				
(a)	2.4	30.7	10.7	14.9
(b)	0.03	0.18	1.7×10^{-4}	0.08
(c)	0.02	0.16	0.2	0.02
Körner and Kramer [41]	2.6	1		
Current algebra (this work)	3.5	1.4	1.7	1.7
Pole model (this work)	1.2	0.87	0.72	0.72
Experiment [31,33]	2.1 ± 0.6	0.8 ± 0.3	0.80 ± 0.35	

predicts larger branching ratios than the pole model. Let us examine this channel by channel.

$\Lambda_c^+ \to p\bar{K}^0$. Equation (2.15) leads to ($f_K = 1.22 f_\pi$)

$$B^{\rm CA} = -\frac{1}{f_K}\frac{m_p + m_{\Sigma^+}}{m_{\Lambda_c^+} - m_{\Sigma^+}} g_A^{\Sigma^+ p} a_{\Lambda_c^+\Sigma^+} = 2.04\times10^{-2}h \ , \quad (4.1)$$

where the axial-vector form factor $g_A^{\Sigma^+ p}$ can be evaluated either directly by the MIT bag model (see Eq. (12) of Ref. [9]) or by applying the Goldberger-Treiman relation together with Eq. (D1). For definiteness, we have used in Eq. (4.1) the bag-model value $g_A^{\Sigma^+ p} = \frac{1}{3}(0.71)$. Adding the pole amplitude (4.1) to the factorizable contribution Eq. (3.19), which vanishes in the soft-meson limit but survives otherwise, yields

$$B^{\rm tot} = B^{\rm fac} + B^{\rm CA} = 0.164h \ , \quad (4.2)$$

which is very close to the pole-model result $B^{\rm tot} = 0.176h$ [See Eq. (3.22)].

As for the s-wave amplitude, it follows from Eq. (2.10) that

$$A^{\rm CA} = \frac{1}{f_K} a_{\Lambda_c^+\Sigma^+} = -4.44\times10^{-2}h \ . \quad (4.3)$$

Therefore,

$$A^{\rm tot} = A^{\rm fac} + A^{\rm CA} = -0.102h \ , \quad (4.4)$$

to be compared with the pole-model PV amplitude $A^{\rm tot} = -1.82\times10^{-2}h$ [Eq. (3.22)]. The discrepancy between current algebra and the pole model for the PV amplitude arises from the fact that the corrections due to $(A - A^{\rm CA})$ given by Eq. (2.11) are already included in the pole-model calculation. Comparing Eq. (2.11) with Eq. (2.9), it is easily seen that the sign of $(A - A^{\rm CA})$ is opposite to $A^{\rm CA}$ and that $|A - A^{\rm CA}| > |A^{\rm CA}|$. This explains why $A^{\rm CA}$ and $A^{\rm pole}$ [Eq. (3.20)] have opposite signs. In other words, the s-wave amplitude of this decay is no longer dominated by the commutator terms. From Eqs. (4.2) and (4.4) we get

$$B(\Lambda_c^+ \to p\bar{K}^0) = 3.5\% \ , \quad \alpha = -0.90 \ . \quad (4.5)$$

Recall that the corresponding predictions in the pole model are 1.2% and -0.49 [Eq. (3.23)].

$\Lambda_c^+ \to \Lambda\pi^+$. Since the commutator term $\langle \Lambda | [Q_5^{\pi^-}, \mathcal{H}_W] | \Lambda_c^+ \rangle$ vanishes, the s-wave amplitude in current algebra receives contributions solely from the factorizable diagrams. We find

$$A^{\rm tot}=A^{\rm fac}=-5.40\times10^{-2}h\ ,$$
$$B^{\rm tot}=B^{\rm fac}+B^{\rm CA}=0.178h-0.0414h=0.137h\ , \tag{4.6}$$

and hence

$$B(\Lambda_c^+\to\Lambda\pi^+)=1.4\%\ ,\quad \alpha=-0.98\ . \tag{4.7}$$

In the pole model $A^{\rm pole}$ is nonvanishing and contributes destructively to the PV amplitude (see Table I). This accounts for why the pole model predicts a smaller branching ratio of 0.87%. Nevertheless, the asymmetry parameter α is predicted by both current algebra and the pole model to be close to -1, in accord with the measured value $-1.0^{+0.4}_{-0.0}$ by CLEO [34] and -0.96 ± 0.42 by ARGUS [35].

$\Lambda_c^+\to\Sigma^0\pi^+$. The current-algebra amplitudes are

$$A^{\rm CA}=\frac{\sqrt{2}}{f_\pi}a_{\Lambda_c^+\Sigma^+}=-7.66\times10^{-2}h\ ,$$

$$B^{\rm CA}=-\frac{1}{f_\pi}\left[\frac{m_{\Sigma^0}+m_{\Sigma^+}}{m_{\Lambda_c^+}-m_{\Sigma^+}}g_A^{\Sigma^0\Sigma^+}a_{\Sigma^+\Lambda_c^+}+\frac{m_{\Lambda_c^+}+m_{\Sigma_c^0}}{m_{\Sigma^0}-m_{\Sigma_c^0}}a_{\Sigma^0\Sigma_c^0}g_A^{\Sigma_c^0\Lambda_c^+}\right]$$
$$=6.39\times10^{-2}h\ , \tag{4.8}$$

where we have used [9]

$$g_A^{\Sigma_c^0\Lambda_c^+}=-\tfrac{1}{2}g_A^{\Sigma^0\Sigma^+}=(\tfrac{2}{3})^{1/2}(0.65)\ . \tag{4.9}$$

Comparing Eq. (4.8) with Eq. (3.24), we see that the relative sign of PC and PV amplitudes flips from the pole model to current algebra. The latter approach predicts

$$B(\Lambda_c^+\to\Sigma^0\pi^+)=1.7\%\ ,\quad \alpha=-0.49\ , \tag{4.10}$$

whereas α is calculated to be 0.83 in the pole model. Consequently, even a measurement of the sign of the up-down asymmetry parameter α in the decay $\Lambda_c^+\to\Sigma^0\pi^+$ (or $\Sigma^+\pi^0$) will help discern various models.

To summarize, since the pole model takes into account the destructive contribution due to $(A-A^{\rm CA})$ for the parity-violating amplitude, its prediction for the branching ratio of $\Lambda_c^+\to B+P$ is smaller than that of current algebra. The two approaches disagree on the sign of the α asymmetry parameter for the decays $\Lambda_c^+\to\Sigma^0\pi^+,\Sigma^+\pi^0$.

B. Comparison with other theoretical calculation

Since current algebra is also the framework employed in Refs. [6–9, 11–13] for the study of $\Lambda_c^+\to B+P$, it is important to elaborate the differences between our current-algebra calculation and others. We first note that the results of Hussain and Scadron [7], though very similar to ours (see Table III), are obtained by ignoring QCD corrections to the Wilson coefficients c_+ and c_-. The inclusion of short-distance QCD effects will enhance, for example, the baryon-baryon matrix elements by a factor of $c_-\approx1.9$, and thus affects significantly their original predictions.

Guberina, Tadić and Trampetić [6], Ebert and Kallies [8(a),8(b)], Cheng [9], Turan and Eeg [13] have done their calculation by using the wave functions of the MIT bag model. The salient features of their results are as follows: (i) the predicted $\Lambda_c^+\to\Lambda\pi^+$ rate is too large by an order of magnitude or even more, as depicted in Table III, and (ii) the ratio of $\Gamma(\Lambda\pi^+)/\Gamma(p\bar{K}^0)$ is considerably larger than unity, ranging from 2.3 to 13, while experimentally it is only (0.41 ± 0.09) [31]. The partial width of $\Lambda\pi^+$ was overestimated before for two reasons. First, the conventional method of evaluating the form factors directly at $q^2=0$ gives too large values, $f_1^{\Lambda_c^+\Lambda}(0)=0.95$, $g_1^{\Lambda_c^+\Lambda}(0)=0.86$ (see, e.g., Ref. [9]). If form factors are first evaluated at maximum q^2 and then extrapolated to $q^2=0$ by assuming a monopole or dipole q^2 dependence (see Sec. III B), they tend to be smaller. For example, $f_1^{\Lambda_c^+\Lambda}(0)=0.46$ and $g_1^{\Lambda_c^+\Lambda}(0)=0.50$ are found in the MIT bag model [26]. The latter approach is more reliable because static-bag and quark-model wave functions best resemble the hadron state at $q^2=(m_i-m_f)^2$. Second, the pole diagrams contribute destructively to the p-wave amplitude [see Table I and Eq. (4.6)] [36]. As a consequence, we find that the branching ratio of $\Lambda_c^+\to\Lambda\pi^+$ is

TABLE IV. Same as Table III except for $\Lambda_c^+\to B+V$ decays.

	$\Lambda_c^+\to p\bar{K}^{*0}$	$\Lambda_c^+\to\Lambda\rho^+$	$\Lambda_c^+\to\Sigma^0\rho^+$	$\Lambda_c^+\to\Sigma^+\rho^0$
Kalinovsky *et al.* [10]				
(a) $g_{K^*}=g_\rho=\sqrt{12\pi}$	20.7	5.9		
(b) $g_{K^*}/g_\rho=m_{K^*}/m_\rho$	2.9	0.6		
Pakvasa *et al.* [11]	0.45	2.8		
Körner and Kramer [41]	10.9–27.3			
Pole model				
(a) $\beta=0$	3.3	2.6	0.19	0.19
(b) $\beta=\frac{3}{4}$	1.8	2.3	0.03	0.03
Experiment	(see Sec. IV B)			

significantly reduced. The fact that the naive expectation of color suppression for the ratio of $\Gamma(\Lambda\pi^+)/\Gamma(p\bar{K}^0)$ is not seen experimentally is not surprising: We have shown in Sec. III D the evidence that the color-suppression mechanism is not operative in $\Lambda_c^+ \to p\phi$, as in the case of charmed-meson decays. Note that the previous predictions made in Refs. [6,8(a),8(b),9,13] for the absolute decay rate of $\Lambda_c^+ \to p\bar{K}^0$ are not far from our present current-algebra results because color suppression [i.e,. $c_2=(2c_+-c_-)/3$] in previous calculations is partly compensated by the large form factors $f_1^{\Lambda_c^+ p}(0) = -\sqrt{3/2}(0.88)$ and $g_1^{\Lambda_c^+ p}(0) = -\sqrt{3/2}(0.77)$ used before. In short, in order to compute the factorizable contributions reliably it is important to employ the large-N_c approach for the Wilson coefficient functions and the $\mathbf{q}=0$ Breit frame for the evaluation of the form factors.

Since the naive estimate of the $\Lambda_c^+ \to \Lambda\pi^+$ decay rate is too large, this motivates Ebert and Kallies [8c] to apply the heavy-quark bag model in which the heavy charm quark occupies the center of the bag so that $v_c \approx 0$. As a result, the numerical values of any quantities involving the charm quark will be drastically reduced. It follows that although $\Lambda_c^+ \to \Lambda\pi^+$ can be accounted for by the heavy-quark bag model, the branching ratio of $p\bar{K}^0$ turns out to be too small. In general, the predicted decay rates of $\Lambda_c^+ \to B+P$ based on this model is too small by at least an order of magnitude [8(c),13] (see Table III). We conclude that the wave function of the charm quark described by the heavy-quark bag model does not work for charmed-baryon decays.

We next turn to the work of Pakvasa, Tuan and Rosen (PTR) [11], Kaur and Khanna (KK) [12]. They employed a large value of c_2 ranging from 0.4 to 0.7 and thus avoided the problem of aforementioned color suppression. However, their c_2 is positive [37], contrary to ours, $c_2 \simeq -0.59$ [Eq. (2.20)] implied by the $1/N_c$ approach. This sign difference will affect the partial width of $\Lambda_c^+ \to p\bar{K}^0(\bar{K}^{*0})$ since its factorizable amplitudes are proportional to c_2. This explains, for example, the large discrepancy between our pole-model prediction of $B(\Lambda_c^+ \to p\bar{K}^{*0})=3.3\%$ and the PTR result 0.45% (both corresponding to $\beta=0$, i.e., the ρ coupling being of the pure F type). While PTR found a large destructive interference between the pole contribution B^{pole} and the factorizable term B^{fac} for the p-wave amplitude, we argue that this interference should be constructive as theory suggests a negative c_2. Unfortunately, the experimental measurement of this decay mode is still quite uncertain: The ratio of $\Gamma(p\bar{K}^{*0})/\Gamma(pK^-\pi^+)$ was previously determined to be 0.18 ± 0.10, 0.35 ± 0.11, and 0.42 ± 0.24, respectively, by Mark II [38]. ACCMOR [30], and R415 [39] Collaborations, and less than 0.59 by ARGUS [40]. Note that the α asymmetry parameter is predicted by PTR to be 0.14 for $p\bar{K}^{*0}$, while we get $\alpha=-0.15$. So a measurement of the up-down asymmetry will furnish a clean test on various models. As to the work of KK, we find that their expression for the commutator terms is too large by a factor of $\sqrt{2}$ (our $f_\pi=132$ MeV). KK obtained a very large branching ratio for $\Lambda_c^+ \to \Sigma^0\pi^+$ due partially to a wrong sign in their formula for B^{pole} and partially to their too large commutator term (see Eq. (16) of Ref. [12]).

In a series of papers, Kalinovsky *et al.* [10] have applied phenomenological chiral Lagrangians to the weak decays of charmed baryons. Strong interactions are described by an SU(4)×SU(4) chiral Lagrangian, while nonleptonic weak interactions are constructed based on certain selection rules. In their scheme, the s-wave amplitude receives contributions from the direct weak-decay diagrams, whereas it arises from the $\frac{1}{2}^-$ pole states in our pole model. The chiral Lagrangian approach predicts too small decay rates for $\Lambda_c^+ \to \Sigma^0\pi^+(\Sigma^+\pi^0)$ (see Table IV), in contradiction with experiment.

Historically, the first systematic and thorough study of two-body nonleptonic decays of charmed baryons was done by Körner, Kramer and Willrodt (KKW) [2]. They evaluated the charmed-baryon decay amplitudes (not just two-body transition elements) directly by using a quark model with U(2,2)-type wave functions. In addition, KKW also used current algebra and an SU(4) model for their calculation. The updated quark-model results presented by Körner and Kramer [41] fit the data well except for the decay $\Lambda_c^+ \to p\bar{K}^{*0}$ which comes out too large.

Finally, it is noteworthy that Deshpande, Trampetić, and Soni [15] and Jarfi *et al.* [16] have investigated baryonic B meson decays using the pole model. Our consideration of charmed-baryon decays shares many features of their calculation. The only crucial difference is that our work is based on the wave functions of the MIT bag model while they employed the harmonic-oscillator quark model.

C. Theoretical uncertainties

We have shown in the present paper that the pole-model predictions for some selective $\Lambda_c^+ \to B+P$ and $B+V$ decay modes are in good agreement with experiment. Nevertheless, we should not consider our predictions as firm results; it is important to discuss and summarize all possible theoretical uncertainties which one may encounter during the course of calculation.

(i) Wave functions of the MIT bag model. We have employed the MIT bag-model wave functions to evaluate baryon-baryon matrix elements and coupling constants. The lightest negative-parity baryon states are obtained from the configurations $(1S_{1/2})^2 1P_{1/2}$ and $(1S_{1/2})^2 1P_{3/2}$, in which two quarks are in the ground $1S_{1/2}$ state and one quark is excited to an $l=1$ state. The MIT bag model can reproduce the qualitative behavior of the spectrum of negative-parity baryon resonances, but is not so successful in reproducing the quantitative features of the observed spectrum [42,43]. It is thus expected that the major uncertainties of the bag-model calculation come from the weak transitions b_{BB^*} and the strong couplings g_{BB^*P} and g_{BB^*V} which involve excited $\frac{1}{2}^-$ baryon states. Furthermore, we have neglected the mixing effect of SU(6) eigenstates (see discussion in Appendix A). Nevertheless, a real advantage of the bag model is that the involved computation is relatively simple and straightforward: All PC and PV baryon matrix elements and relevant couplings are expressed in terms of some bag overlap integrals which in turn can be easily evaluated in a numerical way.

(ii) Coupling constants at nonzero momentum transfer. For simplicity, strong coupling constants have been thus far evaluated only at $q^2=0$, though they should be taken at $q^2=m_P^2$ (or m_V^2) in the pole amplitudes. It is possible that our approximation does not work well for g_{BBK^*}, for instance, since $q^2=m_{K^*}^2$ is not close to the static limit $q^2=0$. In practical calculations, the q^2 dependence of the g_{BBV} coupling constants can be determined by expanding the exponential term in Eq. (D7) to the desired order. For previous efforts along this line, see Ref. [44].

(iii) BBV coupling constants. The vector BBV couplings given by Eq. (D1) are parametrized under SU(3) or SU(4) symmetry in terms of two parameters β and g. While the parameter g is related to the strong $p\rho p$ coupling, β is essentially unknown. We have carried out calculation with two favored values $\beta=0$ and $\frac{3}{4}$. A tensor coupling of the form given by Eq. (2.6) is allowed for the BBV interaction and its contribution to the factorizable amplitudes is summarized in Eq. (2.7). It is not clear to us if the effect of the tensor coupling is negligible.

(iv) Baryon-baryon matrix elements at nonzero momentum transfer. In order to evaluate the baryon matrix element $\langle B_i|\mathcal{H}_w|B_f\rangle$ in the context of the static bag model, it is required to assume that both baryons B_i and B_f are at rest. However, as pointed out by Jarfi *et al.* [16], the three-momentum transfer $\mathbf{k}^2$ in the rest frame of one of the baryons is not small, $\mathbf{k}^2\sim 1\text{GeV}^2$ in charmed baryon decay. A technique for computing the baryon-baryon transition elements at nonzero momentum transfer was developed by Jarfi *et al.* within the harmonic-oscillator quark model. A generalization of this work to the MIT bag model is required.

(v) Contributions of the parity-violating matrix elements to the s-wave amplitude. To compute the s-wave amplitude we have thus far focused on the $\frac{1}{2}^-$ pole terms and ignored the $\frac{1}{2}^+$ pole contributions by assuming that the PV matrix elements $b_{BB'}\sim\langle B(\frac{1}{2}^+)|\mathcal{H}_W^{\rm PV}|B'(\frac{1}{2}^+)\rangle$ is negligible compared to $b_{BB^*}\sim\langle B(\frac{1}{2}^+)|\mathcal{H}_W^{\rm PV}|B^*(\frac{1}{2}^-)\rangle$. It is known that the weak transition $b_{BB'}$ vanishes in the limit of SU(4) symmetry, but this symmetry is badly broken. A calculation in the MIT bag model [9,8c] reveals that $b_{BB'}/a_{BB'}$ ranges from 0.1 to 0.4 for various charmed baryon decays. Corrections to the parity-violating amplitudes due to $b_{BB'}$ should be studied in further detail. It is expected that the PV matrix elements $b_{BB'}$ play an important role in bottom baryon decays since *a priori* they are of the same order of magnitude as PC ones.

(vi) Higher excited baryon resonances and low-lying states with high spin. To estimate the decay amplitudes in the pole model, the ground $\frac{1}{2}^+$ states and low-lying excited $\frac{1}{2}^-$ resonances are assumed to give the most important contributions for s- and p- wave amplitudes, respectively. However, as pointed out by Turan and Eeg [13], because the mass of the charmed baryon B_c is rather large compared to hyperons, excited baryon states with masses close to that of B_c could give significant contributions. For example, in Sec. III E we only consider low-lying (**70**, $L=1$) excited states of Σ^+ for the parity-violating amplitude of $\Lambda_c^+\to p\bar{K}^0$. But, it is possible that higher excited states of Σ^+ or lowest-lying spin $\frac{3}{2}$ states with masses close to Λ_c^+ may contribute sizably to the s-wave decay amplitude. When the wave functions of the MIT bag model are utilized, Turan and Eeg [13] claimed that the lowest-lying spin $\frac{3}{2}$ baryon poles dominate the s-wave amplitude of $\Lambda_c^+\to B+P$ decays [45]. In light of this, further careful work on the effects of higher resonances should be pursued.

V. CONCLUSION AND OUTLOOK

In the present paper we have analyzed the nonleptonic weak decays of charmed baryons within the framework of the pole model. Contrary to current algebra, this approach is operative even if the final-state meson is not soft and of the pseudoscalar type. We have employed the wave function of the MIT bag model to evaluate weak transition elements and strong vertices. Apart from the factorizable contributions, the s-wave amplitudes are approximated by low-lying negative-parity baryon resonances.

For definiteness, we have limited ourselves to some selective decay modes of Λ_c^+ for illustrative purposes. We conclude that (i) the naive expectation of color suppression for $\Lambda_c^+\to p\phi$ and for the ratio of $\Gamma(p\bar{K}^0)/\Gamma(\Lambda\pi^+)$ is not seen by experiment, as in the case of charmed meson decays, (ii) nonspectator (pole) contributions are in general smaller than the factorizable ones for the decay modes which receive contributions from the factorizable diagram, and (iii) the predicted branching ratios based on the wave functions of the heavy-quark bag model are too small. We have compared our work with current algebra and other theoretical calculation. It turns out that current algebra tends to predict larger decay rates for $\Lambda_c^+\to B+P$ decays. Furthermore, we found that the s-wave amplitude of $\Lambda_c^+\to\Sigma^0\pi^+,\Sigma^+\pi^0$ is no longer dominated by the commutator terms. A measurement of the sign of the α asymmetry parameter for the decays $\Lambda_c^+\to\Sigma^0\pi^+$ and $\Sigma^+\pi^0$ will provide a discerning test between current algebra and the pole model.

In the future it is natural to extend our present work to (i) other Cabibbo-favored decay modes, e.g., $\Lambda_c^+\to\Xi K^+,\Sigma^+\eta,\Sigma^+\omega,\Sigma^+\phi,\ldots$, (ii) $\frac{1}{2}^+\to\frac{3}{2}^+ +0^-(1^-)$ transitions, e.g., $\Lambda_c^+\to\Delta^+\bar{K}^0,\Delta^{++}K^-$, $\Sigma(1350)\rho^+,\ldots$, and (iii) nonleptonic weak decays of Σ_c and Ξ_c. New measurements on charmed baryons are now carried out by ARGUS and CLEO, and by several on-going experiments at Fermilab and CERN. With more and more data becoming available in the near future, we are certainly beginning to comprehend the underlying mechanism for charmed baryon decays.

ACKNOWLEDGMENTS

One of us (H.Y.C.) wishes to thank the Physics Department of the Brookhaven National Laboratory, where the major part of this work was done, for their hospitality. This work was supported in part by National Science Council of the Republic of China under Contract No. NSC81-0208-M- 001-06.

APPENDIX A: BAG WAVE FUNCTIONS

In the MIT bag model the quark spatial wave function is given by [23]

$$\psi_{S_{1/2}}=\frac{N_{-1}}{(4\pi R^3)1/2}\begin{bmatrix} ij_0(xr/R)\chi \\ -\sqrt{\epsilon}j_1(xr/R)\sigma\cdot\hat{\mathbf{r}}\chi\end{bmatrix} \equiv \begin{bmatrix} iu(r)\chi \\ v(r)\sigma\cdot\hat{\mathbf{r}}\chi\end{bmatrix} \tag{A1}$$

for the quark in the ground ($1S_{1/2}$) state, and

$$\psi_{P_{1/2}}=\frac{N_1}{(4\pi R^3)1/2}\begin{bmatrix} ij_1(xr/R)\sigma\cdot\hat{\mathbf{r}}\chi \\ \sqrt{\epsilon}j_0(xr/R)\chi\end{bmatrix} \equiv \begin{bmatrix} i\tilde{v}(r)\sigma\cdot\hat{\mathbf{r}}\chi \\ \tilde{u}(r)\chi\end{bmatrix} \tag{A2}$$

as well as [42,43]

$$\psi_{P_{3/2}}=\frac{N_{-2}}{R^{3/2}}\begin{bmatrix} ij_1(xr/R)\phi_{3/2,m} \\ -\sqrt{\epsilon}j_2(xr/R)\sigma\cdot\hat{\mathbf{r}}\phi_{3/2,m}\end{bmatrix} \equiv \begin{bmatrix} i\underset{\sim}{v}(r)\phi_{3/2,m} \\ \underset{\sim}{w}(r)\sigma\cdot\hat{\mathbf{r}}\phi_{3/2,m}\end{bmatrix} \tag{A3}$$

for quarks excited to an $l=1$ state $1P_{1/2}$ and $1P_{3/2}$, respectively, with the j_n' spherical Bessel functions. The normalization factors read

$$N_{-1}=\frac{x^2}{[2\omega(\omega-1)+mR]^{1/2}\sin x},$$
$$N_1=\frac{x^3}{[2\omega(\omega+1)+mR]^{1/2}(\sin x-x\cos x)}, \tag{A4}$$
$$N_{-2}=\frac{x^3}{[2\omega(\omega-2)+mR]^{1/2}(\sin x-x\cos x)},$$

where $\epsilon=(\omega-mR)/(\omega+mR), x=(\omega^2-m^2R^2)^{1/2}$ for a quark of mass m existing within a bag of radius R in mode ω. For convenience, we have dropped in Eq. (A4) the subscript $\kappa(=-1,1,-2)$ of x,ω, and R. The eigenvalue x_κ is determined by the transcendental equations

$$\tan x=\frac{x}{1-mR-(x^2+m^2R^2)^{1/2}},$$
$$\tan x=\frac{x}{1-mR+(x^2+m^2R^2)^{1/2}}, \tag{A5}$$
$$\tan x=\frac{x}{1+x^2/(\omega+mR-3)},$$

for $\kappa=-1,1,-2$, respectively. In Eq. (A3) $\phi_{j,m}$ is the usual spherical harmonic spinor [46]. For the $1P_{3/2}$ quark state,

$$\phi_{3/2,3/2}=\begin{bmatrix} Y_{11} \\ 0\end{bmatrix}, \quad \phi_{3/2,1/2}=\begin{bmatrix} \sqrt{2/3}Y_{10} \\ \sqrt{1/3}Y_{11}\end{bmatrix}, \quad \phi_{3/2,-1/2}=\begin{bmatrix} \sqrt{1/3}Y_{1-1} \\ \sqrt{2/3}Y_{10}\end{bmatrix}. \tag{A6}$$

For the $1S_{1/2}$ and $1P_{1/2}$ states, the spherical harmonic Y_{00} is already absorbed in the normalization factors N_{-1} and N_1.

The low-lying negative-parity noncharmed baryon states (**70**, $L=1$) are made of two quarks in the ground $1S_{1/2}$ state and one quark excited to $1P_{1/2}$ or $1P_{3/2}$. The SU(6) wave functions for the baryon (**70**,$L=1$) states in terms of the $P_{1/2}\equiv(1S_{1/2})^2 1P_{1/2}$ and $P_{3/2}\equiv(1S_{1/2})^2 1P_{3/2}$ wave functions are given by [43]

$$|70,{}^28_{1/2}\rangle=-\tfrac{2}{3}|8,\tfrac{1}{2}^-,P_{3/2}\rangle-\tfrac{2}{3}|8,\tfrac{1}{2}^-,P_{1/2}\rangle_a+\tfrac{1}{3}|8,\tfrac{1}{2}^-,P_{1/2}\rangle_b,$$
$$|70,{}^48_{1/2}\rangle=\tfrac{1}{3}|8,\tfrac{1}{2}^-,P_{3/2}\rangle-\tfrac{2}{3}|8,\tfrac{1}{2}^-,P_{1/2}\rangle_a-\tfrac{2}{3}|8,\tfrac{1}{2}^-,P_{1/2}\rangle_b, \tag{A7}$$
$$|70,{}^210_{1/2}\rangle=-\frac{\sqrt{8}}{3}|10,\tfrac{1}{2}^-,P_{3/2}\rangle-\tfrac{1}{3}|10,\tfrac{1}{2}^-,P_{1/2}\rangle,$$
$$|70,{}^21_{1/2}\rangle=|1,\tfrac{1}{2}^-,P_{1/2}\rangle.$$

It should be stressed that the physical $\frac{1}{2}^-$ resonance states are mixtures of SU(6) eigenstates found in the bag model owing to SU(6) mixings. The mixing matrices are given in Ref. [43]. Nevertheless, we find in practical calculations that the SU(6) mixing effects do not affect the values of weak transition elements and strong vertices in any significant way. Hence, we will neglect such effects for simplicity.

The wave functions for quark states $P_{1/2}$ and $P_{3/2}$ can be worked out from Refs. [42,43]. As an example and also for later purposes, we write down explicitly the wave functions for the $\frac{1}{2}^-$ resonance states of Σ^+:

$$\Sigma^+(8,\tfrac{1}{2}^-,P_{1/2})_a=\frac{1}{\sqrt{54}}\{2[u^\uparrow u^\uparrow \tilde{s}^\downarrow+\tilde{u}^\uparrow u^\uparrow s^\downarrow+u^\uparrow\tilde{u}^\uparrow s^\downarrow]-u^\uparrow u^\downarrow\tilde{s}^\uparrow-\tilde{u}^\uparrow u^\downarrow s^\uparrow-u^\uparrow\tilde{u}^\downarrow s^\uparrow-u^\downarrow u^\uparrow\tilde{s}^\uparrow-\tilde{u}^\downarrow u^\uparrow s^\uparrow-u^\downarrow\tilde{u}^\uparrow s^\uparrow+(13)+(23)\},$$

$$\Sigma^+(8,\tfrac{1}{2}^-,P_{1/2})_b=\frac{1}{\sqrt{54}}\{2[u^\uparrow u^\uparrow \tilde{s}^\downarrow+\tilde{u}^\uparrow u^\downarrow s^\uparrow+u^\downarrow\tilde{u}^\uparrow s^\uparrow]-u^\uparrow u^\downarrow\tilde{s}^\uparrow-\tilde{u}^\uparrow u^\uparrow s^\downarrow-u^\uparrow\tilde{u}^\uparrow s^\downarrow-u^\downarrow u^\uparrow\tilde{s}^\uparrow-\tilde{u}^\downarrow u^\uparrow s^\uparrow-u^\uparrow\tilde{u}^\downarrow s^\uparrow+(13)+(23)\},$$

$$
\begin{aligned}
\Sigma^{+}(8,\tfrac{1}{2}^{-},P_{3/2}) = \frac{1}{\sqrt{108}}\{ & 2[\sqrt{3}u^{\downarrow}u^{\downarrow}\underset{\sim}{s}^{\Big\uparrow}-(u^{\uparrow}u^{\downarrow}+u^{\downarrow}u^{\uparrow})\underset{\sim}{s}^{\uparrow}+u^{\uparrow}u^{\uparrow}\underset{\sim}{s}^{\downarrow}] \\
& -\sqrt{3}u^{\downarrow}\underset{\sim}{u}^{\Big\uparrow}s^{\downarrow}+u^{\uparrow}\underset{\sim}{u}^{\uparrow}s^{\downarrow}+u^{\downarrow}\underset{\sim}{u}^{\uparrow}s^{\uparrow}-u^{\uparrow}\underset{\sim}{u}^{\downarrow}s^{\uparrow} \\
& -\sqrt{3}\underset{\sim}{u}^{\Big\uparrow}u^{\downarrow}s^{\downarrow}+\underset{\sim}{u}^{\uparrow}u^{\uparrow}s^{\downarrow}+\underset{\sim}{u}^{\uparrow}u^{\downarrow}s^{\uparrow}-\underset{\sim}{u}^{\downarrow}u^{\uparrow}s^{\uparrow}+(13)+(23)\} , \\
\Sigma^{+}(10,\tfrac{1}{2}^{-},P_{1/2}) = \frac{1}{\sqrt{54}}\{ & 2[u^{\uparrow}u^{\uparrow}\tilde{s}^{\downarrow}+\tilde{u}^{\downarrow}u^{\uparrow}s^{\uparrow}+u^{\uparrow}\tilde{u}^{\downarrow}s^{\uparrow}]-u^{\uparrow}u^{\downarrow}\tilde{s}^{\uparrow} \\
& -u^{\downarrow}u^{\uparrow}\tilde{s}^{\uparrow}-\tilde{u}^{\uparrow}u^{\downarrow}s^{\uparrow}-\tilde{u}^{\uparrow}u^{\uparrow}s^{\downarrow}-u^{\uparrow}\tilde{u}^{\uparrow}s^{\downarrow}-u^{\downarrow}\tilde{u}^{\uparrow}s^{\uparrow}+(13)+(23)\} , \\
\Sigma^{+}(10,\tfrac{1}{2}^{-},P_{3/2}) = \frac{1}{\sqrt{54}}\{ & \sqrt{3}[u^{\downarrow}u^{\downarrow}\underset{\sim}{s}^{\Big\uparrow}+u^{\downarrow}\underset{\sim}{u}^{\Big\uparrow}s^{\downarrow}+\underset{\sim}{u}^{\Big\uparrow}u^{\downarrow}s^{\downarrow}] \\
& -(u^{\uparrow}u^{\downarrow}+u^{\downarrow}u^{\uparrow})\underset{\sim}{s}^{\uparrow}+u^{\uparrow}u^{\uparrow}\underset{\sim}{s}^{\downarrow}-u^{\uparrow}\underset{\sim}{u}^{\uparrow}s^{\downarrow}-u^{\downarrow}\underset{\sim}{u}^{\uparrow}s^{\uparrow} \\
& +u^{\uparrow}\underset{\sim}{u}^{\downarrow}s^{\uparrow}-\underset{\sim}{u}^{\uparrow}u^{\uparrow}s^{\downarrow}-\underset{\sim}{u}^{\uparrow}u^{\downarrow}s^{\uparrow}+\underset{\sim}{u}^{\downarrow}u^{\uparrow}s^{\uparrow}+(13)+(23)\} ,
\end{aligned}
\tag{A8}
$$

where the $1P_{1/2}(1P_{3/2})$ quark is denoted by a tilde (undertilde), the $s_z=\frac{3}{2}$ quark state is marked by $\underset{\sim}{q}^{\Big\uparrow}$, and (ij) means permutation for the quark in place i with the quark in place j. The wave function of the $\frac{1}{2}^{-}$ charmed baryon can be constructed in the same way. However, since the charm quark is heavy, it should be treated differently: The charm quark in the low-lying resonance states does not get excited. Consequently, the wave function of, say, $\Sigma_c^0(\frac{1}{2}^{-})$, has a simple expression, for example,

$$
\begin{aligned}
\Sigma_c^0(8,\tfrac{1}{2}^{-},P_{1/2})_a = \frac{1}{\sqrt{12}}\{ & 2(\tilde{d}^{\uparrow}d^{\uparrow}c^{\downarrow}+d^{\uparrow}\tilde{d}^{\uparrow}c^{\downarrow})-\tilde{d}^{\uparrow}d^{\downarrow}c^{\uparrow} \\
& -d^{\downarrow}\tilde{d}^{\uparrow}c^{\uparrow}-\tilde{d}^{\downarrow}d^{\uparrow}c^{\uparrow}-d^{\uparrow}\tilde{d}^{\downarrow}c^{\uparrow}\} .
\end{aligned}
\tag{A9}
$$

To fix the relative sign of the coupling constants, form factors, parity-conserving and -violating matrix elements, it is very important to employ the baryon wave function consistently. In the present paper, we use the isospin baryon-pseudoscalar coupling convention given in Ref. [47] (see Appendix D) to fix the sign of the baryon wave functions. In the following, we list those wave functions relevant to our purposes:

$$
\begin{aligned}
& p=\frac{1}{\sqrt{3}}[uud\chi_s+(13)+(23)] , \\
& \Sigma^{+}=-\frac{1}{\sqrt{3}}[uus\chi_s+(13)+(23)] , \\
& \Sigma^{0}=\frac{1}{\sqrt{6}}[(uds+dus)\chi_s+(13)+(23)] , \\
& \Lambda^{0}=-\frac{1}{\sqrt{6}}[(uds-dus)\chi_A+(13)+(23)] , \\
& \Lambda_c^{+}=-\frac{1}{\sqrt{2}}[(udc-duc)\chi_s+(13)+(23)] , \\
& \Sigma_c^{+}=\frac{1}{\sqrt{2}}[(udc+duc)\chi_s+(13)+(23)] , \\
& \Sigma_c^{0}=ddc\chi_s ,
\end{aligned}
\tag{A10}
$$

where $abc\chi_s=(2a^{\uparrow}b^{\uparrow}c^{\downarrow}-a^{\uparrow}b^{\downarrow}c^{\uparrow}-a^{\downarrow}b^{\uparrow}c^{\uparrow})/\sqrt{6}$, $abc\chi_A=(a^{\uparrow}b^{\downarrow}c^{\uparrow}-a^{\downarrow}b^{\uparrow}c^{\uparrow})/\sqrt{2}$. Note a negative relative sign between the wave function of Σ^{+} and p.

APPENDIX B: PARITY-CONSERVING MATRIX ELEMENTS

In terms of the large and small components $u(r)$ and $v(r)$ of the $1S_{1/2}$ quark wave function [see Eq. (A1)], the matrix element of the two-quark operators $V_\mu(x)=\bar{q}'\gamma_\mu q$ and $A_\mu(x)=\bar{q}'\gamma_\mu\gamma_5 q$ are given by

$$
\begin{aligned}
& \langle q'|V_0|q\rangle=u'u+v'v , \\
& \langle q'|A_0|q\rangle=-i(u'v-v'u)\boldsymbol{\sigma}\cdot\hat{\mathbf{r}} , \\
& \langle q'|\mathbf{V}|q\rangle=-(u'v+v'u)\boldsymbol{\sigma}\times\hat{\mathbf{r}}-i(u'v-v'u)\hat{\mathbf{r}} , \\
& \langle q'|\mathbf{A}|q\rangle=(u'u-v'v)\boldsymbol{\sigma}+2v'v\hat{\mathbf{r}}\boldsymbol{\sigma}\cdot\hat{\mathbf{r}} .
\end{aligned}
\tag{B1}
$$

The four-quark operator $O_-(x)$ given by Eq. (2.17) can be written as $O_-(x)=6[(\bar{s}c)_1(\bar{u}d)_2-(\bar{s}d)_1(\bar{u}c)_2]$, where the subscript i indicates that the quark operator acts only on the ith quark in the baryon wave function. It follows from Eq. (B1) that the parity-conserving (PC) matrix elements have the form

$$
\begin{aligned}
& \int r^2dr\langle q_1'q_2'|(\bar{s}c)_1(\bar{u}d)_2|q_1q_2\rangle \\
& \qquad =(-X_1+X_2)-\tfrac{1}{3}(X_1+3X_2)\boldsymbol{\sigma}_1\cdot\boldsymbol{\sigma}_2 , \\
& \int r^2dr\langle q_1'q_2'|(\bar{s}d)_1(\bar{u}c)_2|q_1q_2\rangle \\
& \qquad =(X_1+X_2)-\tfrac{1}{3}(-X_1+3X_2)\boldsymbol{\sigma}_1\cdot\boldsymbol{\sigma}_2 ,
\end{aligned}
\tag{B2}
$$

where X_1 and X_2 are the four-quark overlap bag integrals [13]

$$
\begin{aligned}
& X_1=\int_0^R r^2dr(u_dv_c-v_du_c)(u_sv_u-v_su_u) , \\
& X_2=\int_0^R r^2dr(u_du_c+v_dv_c)(u_su_u+v_sv_u) ,
\end{aligned}
\tag{B3}
$$

and use of $\int d\Omega(\boldsymbol{\sigma}_1\cdot\hat{r}\boldsymbol{\sigma}_2\cdot\hat{r})=\frac{1}{3}\int d\Omega(\boldsymbol{\sigma}_1\cdot\boldsymbol{\sigma}_2)$ has been made. After evaluating the matrix elements $\langle\boldsymbol{\sigma}_1\cdot\boldsymbol{\sigma}_2\rangle$, we find the PC bag matrix elements to be

$$
\begin{aligned}
& \langle\Sigma^{+}|O_-^{\mathrm{PC}}|\Lambda_c^{+}\rangle=\langle\Sigma_c^{0}|O_-^{\mathrm{PC}}|\Lambda^{0}\rangle \\
& \qquad =-\frac{4}{\sqrt{6}}(X_1+3X_2)(4\pi) , \\
& \langle\Sigma_c^{+}|O_-^{\mathrm{PC}}|\Sigma^{+}\rangle=\langle\Sigma_c^{0}|O_-^{\mathrm{PC}}|\Sigma^{0}\rangle \\
& \qquad =\frac{2\sqrt{2}}{3}(-X_1+9X_2)(4\pi) .
\end{aligned}
\tag{B4}
$$

Note that the sign of each PC matrix element is fixed by the baryon wave functions given by Eq. (A10).

APPENDIX C: PARITY-VIOLATING MATRIX ELEMENTS

The evaluation of the parity-violating (PV) matrix elements for $\frac{1}{2}^+-\frac{1}{2}^-$ transitions is much more involved. From Eq. (A1) it is straightforward to show that

$$\begin{aligned}\langle \tilde{q}'_1 q'_2|V\cdot A + A\cdot V|q_1q_2\rangle = & -i(\tilde{v}'v-\tilde{u}'u)_1(u'u+v'v)_2+i(\tilde{u}'v+\tilde{v}'u)_1(u'v-v'u)_2\\ & -i(\boldsymbol{\sigma}_1\cdot\boldsymbol{\sigma}_2)[(\tilde{u}'u+\tilde{v}'v)_1(u'u-v'v)_2-(\tilde{v}'u-\tilde{u}'v)_1(u'v+v'u)_2]\\ & -2i(\boldsymbol{\sigma}_1\cdot\hat{\mathbf{r}}\boldsymbol{\sigma}_2\cdot\hat{\mathbf{r}})[(\tilde{v}'u)_1(u'v)_2-(\tilde{u}'v)_1(v'u)_2+(\tilde{u}'u)_1(v'v)_2-(\tilde{v}'v)_1(u'u)_2] \qquad (C1)\end{aligned}$$

and

$$\begin{aligned}\langle \underset{\sim}{q}'_1 q'_2|V\cdot A + A\cdot V|q_1q_2\rangle = & -(\boldsymbol{\sigma}_1\times\boldsymbol{\sigma}_2)\cdot\hat{\mathbf{r}}[(\underset{\sim}{v}'v+\underset{\sim}{w}'u)_1(u'u-v'v)_2-(\underset{\sim}{v}'u-\underset{\sim}{w}'v)_1(u'v+v'u)_2]\\ & +i(\boldsymbol{\sigma}_1-\boldsymbol{\sigma}_2)\cdot\hat{\mathbf{r}}[\underset{\sim}{v}'u+\underset{\sim}{w}'v)_1(u'v-v'u)_2-(\underset{\sim}{v}'v-\underset{\sim}{w}'u)_1(u'u+v'v)_2] \ . \qquad (C2)\end{aligned}$$

Note that

$$\begin{aligned}\langle q_1q_2|V\cdot A + A\cdot V|\tilde{q}'_1q'_2\rangle &= -\langle \tilde{q}'_1q'_2|V\cdot A + A\cdot V|q_1q_2\rangle \ ,\\ \langle q_1q_2|V\cdot A + A\cdot V|\underset{\sim}{q}'_1q'_2\rangle &= -\langle \underset{\sim}{q}'_1q'_2|V\cdot A + A\cdot V|q_1q_2\rangle \ . \end{aligned} \qquad (C3)$$

In the following we will consider the PV matrix elements $\langle \Sigma^+(8,P_{1/2})_a|O_-^{\rm PV}|\Lambda_c^+\rangle$ and $\langle \Sigma^+(8,P_{3/2})|O_-^{\rm PV}|\Lambda_c^+\rangle$ as an example of evaluation. First, we note that

$$\langle \Sigma^+(8,P_{1/2})_a|(\bar{s}c)(\bar{u}d)|\Lambda_c^+\rangle = 6\langle \Sigma^+(8,P_{1/2})_a|(\bar{s}c)_3(\bar{u}d)_1|\Lambda_c^+\rangle + 6\langle \Sigma^+(8,P_{1/2})_a|(\bar{u}d)_1(\bar{s}c)_3|\Lambda_c^+\rangle \ . \qquad (C4)$$

The flavor operator in the first term on the right-hand side (RHS) of Eq. (C4) is of the form $b_{1u}^\dagger b_{1d} b_{3\tilde{s}}^\dagger b_{3c}$, where $b_{3\tilde{s}}^\dagger$ denotes a $1P_{1/2}$ strange-quark construction operator acting on the third quark in the baryon wave function. Likewise, we have the operator $b_{1\tilde{u}}^\dagger b_{1d} b_{3s}^\dagger b_{3c}$ in the second term. Using the relation

$$\boldsymbol{\sigma}_1\cdot\boldsymbol{\sigma}_2=\tfrac{1}{2}(\sigma_{1+}\sigma_{2-}+\sigma_{1-}\sigma_{2+})+\sigma_{1z}\sigma_{2z} \qquad (C5)$$

with $\sigma_\pm=\sigma_x\pm i\sigma_y$, and the wave function of $\Sigma^+(8,P_{1/2})_a$ and Λ_c^+ given before, we find

$$\begin{aligned}\int d\Omega\langle \Sigma^+(8,P_{1/2})_a|b_{1u}^\dagger b_{1d}b_{3\tilde{s}}^\dagger b_{3c}(\boldsymbol{\sigma}_1\cdot\boldsymbol{\sigma}_3)|\Lambda_c^+\rangle &= -\frac{1}{3\sqrt{2}}(4\pi) \ ,\\ \int d\Omega\langle \Sigma^+(8,P_{1/2})_a|b_{1\tilde{u}}^\dagger b_{1d}b_{3s}^\dagger b_{3c}(\boldsymbol{\sigma}_1\cdot\boldsymbol{\sigma}_3)|\Lambda_c^+\rangle &= -\frac{1}{3\sqrt{2}}(4\pi) \ . \end{aligned} \qquad (C6)$$

It follows from Eqs. (C4), (C6), and (C1) that

$$\begin{aligned}\langle \Sigma^+(8,P_{1/2})_a|(\bar{s}c)(\bar{u}d)|\Lambda_c^+\rangle = & \, i\frac{8\pi}{\sqrt{2}}[\tfrac{1}{3}(\tilde{v}_sv_cu_u^2-\tilde{u}_su_cv_u^2)-(\tilde{v}_sv_cv_u^2-\tilde{u}_su_cu_u^2)-\tfrac{4}{3}(\tilde{v}_su_c-\tilde{u}_sv_c)u_uv_u]\\ & +i\frac{8\pi}{\sqrt{2}}[\tfrac{1}{3}(\tilde{v}_uv_uu_su_c-\tilde{u}_uu_uv_sv_c-\tilde{v}_uu_uu_sv_c+\tilde{u}_uv_uv_su_c)\\ & +(\tilde{u}_uu_uu_su_c-\tilde{v}_uv_uv_sv_c+\tilde{u}_uv_uu_sv_c-\tilde{v}_uu_uv_su_c)] \ . \qquad (C7)\end{aligned}$$

Repeating a similar evaluation for $\langle \Sigma^+(8,P_{1/2})_a|(\bar{s}d)(\bar{u}c)|\Lambda_c^+\rangle$, we then obtain

$$\begin{aligned}&\langle \Sigma^+(8,P_{1/2})_a|O_-^{\rm PV}|\Lambda_c^+\rangle\\ &\quad = i2\sqrt{2}(4\pi)(-\tfrac{1}{3}\tilde{X}_1+\tilde{X}_2+\tfrac{1}{3}\tilde{X}_{1s}+\tilde{X}_{2s}) \qquad (C8)\end{aligned}$$

with

$$\begin{aligned}\tilde{X}_1&=\int {}^2dr(u_uv_c-v_uu_c)(\tilde{v}_uu_s+\tilde{u}_uv_s) \ ,\\ \tilde{X}_2&=\int r^2dr(u_uu_c+v_uv_c)(\tilde{u}_uu_s-\tilde{v}_uv_s) \ ,\\ \tilde{X}_{1s}&=\int r^2dr(u_uv_c-v_uu_c)(\tilde{u}_sv_u+\tilde{v}_su_u) \ ,\\ \tilde{X}_{2s}&=\int r^2dr(u_uu_c+v_uv_c)(\tilde{u}_su_u-\tilde{v}_sv_u) \ . \end{aligned} \qquad (C9)$$

For the matrix element of $\Sigma^+(8,P_{3/2})-\Lambda_c^+$ transition, we note that the $\hat{r}_x$ and $\hat{r}_y$ components of $(\boldsymbol{\sigma}_1\times\boldsymbol{\sigma}_2)\cdot\hat{\mathbf{r}}$ and $(\boldsymbol{\sigma}_1-\boldsymbol{\sigma}_2)\cdot\hat{\mathbf{r}}$ make no contributions, so that

$$\begin{aligned}(\boldsymbol{\sigma}_1\times\boldsymbol{\sigma}_2)\cdot\hat{\mathbf{r}}&\rightarrow\frac{i}{2}(\sigma_{1+}\sigma_{2-}-\sigma_{1-}\sigma_{2+})\hat{\mathbf{r}}_z \ ,\\ (\boldsymbol{\sigma}_1-\boldsymbol{\sigma}_2)\cdot\hat{\mathbf{r}}&\rightarrow(\sigma_{1z}-\sigma_{2z})\hat{\mathbf{r}}_z \ . \end{aligned} \qquad (C10)$$

The orthogonal condition

$$\int d\Omega\, Y_{l'm'}^*(\theta,\phi)Y_{l,m}(\theta,\phi)=\delta_{ll'}\delta_{mm'} \qquad (C11)$$

together with

$$\int d\Omega\,\hat{\mathbf{r}}_z\phi_{3/2,1/2}^\dagger\begin{bmatrix}1\\0\end{bmatrix}=\int d\Omega\,\hat{\mathbf{r}}_z\phi_{3/2,-1/2}^\dagger\begin{bmatrix}0\\1\end{bmatrix}=\tfrac{2}{3}\sqrt{2\pi} \qquad (C12)$$

leads to

$$\begin{aligned}
&\int d\Omega\langle\Sigma^+(8,P_{3/2})|b^\dagger_{1u}b_{1d}b^\dagger_{3s}b_{3c}(\sigma_3\times\sigma_1)\cdot\hat{\mathbf{r}}|\Lambda_c^+\rangle=i\frac{2}{27}\sqrt{2\pi}\ ,\\
&\int d\Omega\langle\Sigma^+(8,P_{3/2})|b^\dagger_{1u}b_{1d}b^\dagger_{3s}b_{3c}(\sigma_3-\sigma_1)\cdot\hat{\mathbf{r}}|\Lambda_c^+\rangle=\frac{2}{27}\sqrt{2\pi}\ ,\\
&\int d\Omega\langle\Sigma^+(8,P_{3/2})|b^\dagger_{1u}b_{1d}b^\dagger_{3s}b_{3c}(\sigma_1\times\sigma_3)\cdot\hat{\mathbf{r}}|\Lambda_c^+\rangle=-i\frac{1}{27}\sqrt{2\pi}\ ,\\
&\int d\Omega\langle\Sigma^+(8,P_{3/2})|b^\dagger_{1u}b_{1d}b^\dagger_{3s}b_{3c}(\sigma_1-\sigma_3)\cdot\hat{\mathbf{r}}|\Lambda_c^+\rangle=-\frac{1}{27}\sqrt{2\pi}\ .
\end{aligned}\tag{C13}$$

After some manipulation we get

$$\langle\Sigma^+(8,P_{3/2})|O_-^{\rm PV}|\Lambda_c^+\rangle=-i\tfrac{8}{9}\sqrt{2\pi}(\underset{\sim}{X}_1+2\underset{\sim}{X}_{1s})\ ,\tag{C14}$$

where

$$\begin{aligned}
\underset{\sim}{X}_1&=\int r^2dr(u_uv_c-v_uu_c)(\underset{\sim}{v}_uu_s+\underset{\sim}{w}_uv_s)\ ,\\
\underset{\sim}{X}_{1s}&=\int r^2dr(u_uv_c-v_uu_c)(\underset{\sim}{w}_sv_u+\underset{\sim}{v}_su_u)\ .
\end{aligned}\tag{C15}$$

The remaining $\Sigma^+(\frac{1}{2}^-)-\Lambda_c^+$ matrix elements are found to be

$$\begin{aligned}
\langle\Sigma^+(8,P_{1/2})_b|O_-^{\rm PV}|\Lambda_c^+\rangle&=i2\sqrt{2}(4\pi)\\
&\quad\times(\tfrac{2}{3}\tilde{X}_1+\tfrac{1}{3}\tilde{X}_{1s}+\tilde{X}_{2s})\ ,\\
\langle\Sigma^+(10,P_{1/2})|O_-^{\rm PV}|\Lambda_c^+\rangle&=i2\sqrt{2}(4\pi)\\
&\quad\times(-\tfrac{1}{3}\tilde{X}_1-\tilde{X}_2+\tfrac{1}{3}\tilde{X}_{1s}+\tilde{X}_{2s})\ ,\\
\langle\Sigma^+(10,P_{3/2})|O_-^{\rm PV}|\Lambda_c^+\rangle&=i\tfrac{8}{9}\sqrt{4\pi}(\underset{\sim}{X}_1-\underset{\sim}{X}_{1s})\ .
\end{aligned}\tag{C16}$$

For completeness, we also summarize the PV matrix elements which are relevant to the present paper:

$$\begin{aligned}
&\langle\Sigma_c^0(8,P_{1/2})_a|O_-^{\rm PV}|\Lambda^0\rangle=i2\sqrt{3}(4\pi)(\tfrac{1}{3}\tilde{X}'_1-\tilde{X}'_2)\ ,\\
&\langle\Sigma_c^0(8,P_{1/2})_b|O_-^{\rm PV}|\Lambda^0\rangle=i2\sqrt{3}(4\pi)(-\tfrac{2}{3}\tilde{X}'_1)\ ,\\
&\langle\Sigma_c^0(10,P_{1/2})|O_-^{\rm PV}|\Lambda^0\rangle=i2\sqrt{3}(4\pi)(\tfrac{1}{3}\tilde{X}'_1+\tilde{X}'_2)\ ,\\
&\langle\Sigma_c^0(8,P_{3/2})|O_-^{\rm PV}|\Lambda^0\rangle=i\frac{4\sqrt{6}}{9}\sqrt{4\pi}(\underset{\sim}{X}'_1)\ ,\\
&\langle\Sigma_c^0(10,P_{3/2})|O_-^{\rm PV}|\Lambda^0\rangle=i\frac{4\sqrt{6}}{9}\sqrt{4\pi}(-\underset{\sim}{X}'_1)\ ,
\end{aligned}\tag{C17}$$

for $\Sigma_c^0(\frac{1}{2}^-)-\Lambda^0$ transitions, where $\tilde{X}'_i$ and $\underset{\sim}{X}'_i$ are obtained from $\tilde{X}_i$ and $\underset{\sim}{X}_i$ by the replacement $s\leftrightarrow c, d\leftrightarrow u$,

$$\begin{aligned}
&\langle\Sigma_c^0(8,P_{1/2})_a|O_-^{\rm PV}|\Sigma^0\rangle=i2(4\pi)(\tfrac{1}{3}\tilde{X}'_1+3\tilde{X}'_2)\ ,\\
&\langle\Sigma_c^0(8,P_{1/2})_b|O_-^{\rm PV}|\Sigma^0\rangle=i2(4\pi)(-\tfrac{2}{3}\tilde{X}'_1)\ ,\\
&\langle\Sigma_c^0(10,P_{1/2})|O_-^{\rm PV}|\Sigma_0\rangle=i2(4\pi)(\tfrac{1}{3}\tilde{X}'_1-3\tilde{X}'_2)\ ,\\
&\langle\Sigma_c^0(8,P_{3/2})|O_-^{\rm PV}|\Sigma^0\rangle=i\tfrac{8}{9}\sqrt{2\pi}(\underset{\sim}{X}'_1)\ ,\\
&\langle\Sigma_c^0(10,P_{3/2})|O_-^{\rm PV}|\Sigma^0\rangle=i\tfrac{8}{9}\sqrt{2\pi}(-\underset{\sim}{X}'_1)\ ,
\end{aligned}\tag{C18}$$

for $\Sigma_c^0(\frac{1}{2}^-)-\Sigma^0$ transitions, and

$$\langle\Sigma_c^+(\tfrac{1}{2}^-)|O_-^{\rm PV}|\Sigma^+\rangle=-\langle\Sigma_c^0(\tfrac{1}{2}^-)|O_-^{\rm PV}|\Sigma^0\rangle\ .\tag{C19}$$

Applying Eq. (A7) enables us to write down the PV baryon matrix elements in terms of the SU(6) $\frac{1}{2}^-$ baryon eigenstates.

APPENDIX D: STRONG MESON-BARYON COUPLING CONSTANTS

The baryon-pseudoscalar meson BBP coupling constants can be related to the axial-vector form factors via the Goldberger-Treiman (GT) relation, which are then evaluated using the MIT bag model. However, we adopt in this paper the method of Ref. [48] in which the BBP couplings are evaluated more accurately by employing the null result of Coleman and Glashow for the tadpole-type symmetry breaking and applying the generalized GT relation to take into account SU(4)-symmetry breaking. The results relevant for our purposes are [48]

$$\begin{aligned}
&g_{\Sigma^+p\bar{K}^0}=4.9\ ,\quad g_{\Sigma^+\Lambda^0\pi^+}=11.8\ ,\quad g_{\Sigma^+\Xi^0K^+}=25.6\ ,\\
&g_{\Sigma^+\Sigma^+\pi^0}=-g_{\Sigma^+\Sigma^0\pi^+}=13.3\ ,\\
&g_{\Sigma_c^+\Lambda_c^+\pi^0}=g_{\Sigma_c^0\Lambda_c^+\pi^+}=23.5\ ,
\end{aligned}\tag{D1}$$

where the sign of the coupling constants is fixed by the isospin coupling convention given in Ref. [47]. For the BBV coupling constants, we will only consider the vector interaction of the vector meson with baryons and neglect the tensor one given by Eq. (2.6). Following Ref. [10], the vector BBV coupling constants under SU(3) or SU(4) symmetry read

$$\begin{aligned}
&g_{\Sigma^+p\bar{K}^{*0}}=\frac{1}{\sqrt{2}}g_{K^*}(2\beta-1)\ ,\\
&g_{\Sigma^+\Lambda^0\rho^+}=\frac{1}{\sqrt{3}}g_\rho\beta\ ,\quad g_{\Sigma^+\Xi^0K^{*+}}=\frac{1}{\sqrt{2}}g_{K^*}\ ,\\
&g_{\Sigma^+\Sigma^+\rho^0}=-g_{\Sigma^+\Sigma^0\rho^+}=-g_\rho(\beta-1)\ ,\\
&g_{\Sigma_c^+\Lambda_c^+\rho^0}=g_{\Sigma_c^0\Lambda_c^+\rho^+}=\frac{1}{\sqrt{3}}g_\rho\beta\ ,
\end{aligned}\tag{D2}$$

where the parameter β measures the mixing of the F- and D-type couplings. If $\beta=0$ is assumed, the BBV coupling constant will be of pure F type. It has been advocated that $\beta=0$ is a good approximation because the ρ meson generates isospin [11]. However, Kalinovsky *et al.* [10] argued that the Okuho-Zweig-Iizuka (OZI) rule in the scheme of ideal mixing of the vector mesons $\omega-\phi$ is satisfied by $\beta=\frac{3}{4}$. In this paper we shall use both $\beta=0$ and $\beta=\frac{3}{4}$ for numerical calculation.

To evaluate the s-wave amplitudes we also need to know the B^*BP and B^*BV coupling constants (B^*:$\frac{1}{2}^-$

resonance). We shall use the generalized GT relation to estimate the B^*BP interaction [49]

$$g_{B^*BP}=\sqrt{2}\frac{m_{B^*}-m_B}{f_P}g^A_{B^*B}\ , \qquad \text{(D3)}$$

where f_P is the decay constant of the pseudoscalar meson P, and $g^A_{B^*B}$ is the axial-vector coupling constant evaluated at $q^2=0$. It has been shown that the generalized GT relation, when applied to the $\Lambda^*\Sigma^+\pi^+$ interaction, is in good agreement with experiment [50]. Note that $g_{BB^*P}=g_{B^*BP}$, while $g^A_{BB^*}=-g^A_{B^*B}$. In the static limit, we find

$$g^A_{B^*B}=\int r^2dr(\tilde{v}v-\tilde{u}u)\int d\Omega\langle B^*|b^\dagger_q b_q|B\rangle + \int r^2dr(\underline{v}v-\underline{w}u)\int d\Omega\langle B^*|b^\dagger_{\underline{q}} b_q(\sigma_z\hat{r}_z)|B\rangle\ . \qquad \text{(D4)}$$

As for the couplings B^*BV, we note that the reduction formula

$$\langle A\rho^a(q)|B\rangle = i\int d^4x e^{iq\cdot x}(\Box+m^2_\rho)\langle A|\rho^a_\mu(x)|B\rangle\epsilon^{*\mu}\ , \qquad \text{(D5)}$$

where ϵ_μ is the polarization vector of the ρ meson, together with the ρ-meson equation of motion

$$(\Box+m^2_\rho)\langle A|\rho^a_\mu(x)|B\rangle = f_\rho\langle A|\tfrac{1}{2}\bar{q}(x)\gamma_\mu\lambda^a q(x)|B\rangle \qquad \text{(D6)}$$

leads to [51]

$$\langle A\rho^a_\mu(q)|B\rangle = if_\rho\int d^4x e^{iq\cdot x} \times\langle A|\tfrac{1}{2}\bar{q}(x)\gamma_\mu\lambda^a q(x)|B\rangle\epsilon^{*\mu}\ . \qquad \text{(D7)}$$

When $A=B=N$, f_ρ at $q^2=0$ is nothing but the strong $NN\rho$ coupling constant $g_{NN\rho}$. When $A=N^*, B=N$, then $g_{N^*N\rho}$ is related to $g_{NN\rho}$ via Eq. (D7). For simplicity, we will limit ourselves to the static limit, i.e., $q_\mu\to 0$, where only the spatial part of V_μ contributes to f_ρ. We obtain

$$g_{B^*B\rho^+}=g_{BB\rho^+}\left[\tilde{Y}_2\int d\Omega\langle B^*|b^\dagger_{\bar{u}} b_d\sigma_z|B\rangle + \underline{Y}_1\int d\Omega\langle B^*|b^\dagger_{\underline{u}} b_d\hat{r}_z|B\rangle\right]\ ,$$
$$g_{B^*B\bar{K}^{*0}}=g_{BB\bar{K}^{*0}}\left[\tilde{Y}_{2s}\int d\Omega\langle B^*|b^\dagger_{\bar{s}} b_d\sigma_z|B\rangle + \underline{Y}_{1s}\int d\Omega\langle B^*|b^\dagger_{\underline{s}} b_d\hat{r}_z|B\rangle\right]\ , \qquad \text{(D8)}$$

where

$$\underline{Y}_1=\int r^2dr(\underline{w}_u u_u-\underline{v}_u v_u)\ ,$$
$$\underline{Y}_{1s}=\int r^2dr(\underline{w}_s u_u-\underline{v}_s v_u)\ ,$$
$$\tilde{Y}_2=\int r^2dr(\tilde{u}_u u_u+\tfrac{1}{3}\tilde{v}_u v_u)\ ,$$
$$\tilde{Y}_{2s}=\int r^2dr(\tilde{u}_s u_u+\tfrac{1}{3}\tilde{v}_s v_u)\ . \qquad \text{(D9)}$$

As an illustration, let us consider the coupling constants $g_{\Sigma^+(^28)\Sigma^0\pi^+}$ and $g_{\Sigma^+(^28)\Sigma^0\rho^+}$, where $\Sigma^+(^28)$ is the shorthand notation for $\Sigma^+(70,\frac{1}{2}^-,{}^28_{1/2})$. From Eqs. (A8) and (A10) we get the nonvanishing matrix elements

$$\int d\Omega\langle\Sigma^+(8,P_{1/2})_a|b^\dagger_{\bar{u}} b_d|\Sigma^0\rangle=\frac{2}{\sqrt{6}}(4\pi)\ ,$$
$$\int d\Omega\langle\Sigma^+(8,P_{1/2})_b|b^\dagger_{\bar{u}} b_d|\Sigma^0\rangle=-\frac{1}{\sqrt{6}}(4\pi)\ , \qquad \text{(D10)}$$
$$\int d\Omega\langle\Sigma^+(10,P_{1/2})|b^\dagger_{\bar{u}} b_d|\Sigma^0\rangle=-\frac{1}{\sqrt{6}}(4\pi)\ ,$$

and

$$\int d\Omega\langle\Sigma^+(8,P_{1/2})_a|b^\dagger_{\bar{u}} b_d\sigma_z|\Sigma^0\rangle=\frac{4}{3\sqrt{6}}(4\pi)\ ,$$
$$\int d\Omega\langle\Sigma^+(8,P_{1/2})_b|b^\dagger_{\bar{u}} b_d\sigma_z|\Sigma^0\rangle=-\frac{5}{3\sqrt{6}}(4\pi)\ , \qquad \text{(D11)}$$
$$\int d\Omega\langle\Sigma^+(8,P_{3/2})|b^\dagger_{\underline{u}} b_d\hat{r}_z|\Sigma^0\rangle=\frac{2}{9\sqrt{6}}\sqrt{4\pi}\ .$$

It follows from Eqs. (A7), (D3), (D4), and (D8) that

$$g_{\Sigma^+(^28)\Sigma^0\pi^+}=\frac{5(4\pi)}{3\sqrt{6}}\frac{m_{\Sigma^+(^28)}-m_{\Sigma^0}}{f_\pi}\tilde{Y}_1\ ,$$
$$g_{\Sigma^+(^28)\Sigma^0\rho^+}=-g_{\Sigma^+\Sigma^0\rho^+}\left[\frac{4}{27\sqrt{6}}\sqrt{4\pi}\underline{Y}_1+\frac{13}{9\sqrt{6}}(4\pi)\tilde{Y}_2\right]\ , \qquad \text{(D12)}$$

where

$$\tilde{Y}_1=\int r^2dr(\tilde{u}_u u_u-\tilde{v}_u v_u)\ ,$$
$$\tilde{Y}_{1s}=\int r^2dr(\tilde{u}_s u_u-\tilde{v}_s v_u)\ . \qquad \text{(D13)}$$

[1] For a review of charmed baryons, see J. G. Körner and H. W. Siebert, Annu. Rev. Nucl. Part. Sci. (to be published); S. R. Klein, Int. J. Mod. Phys. A **5**, 1457 (1990).

[2] J. G. Körner, G. Kramer, and J. Willrodt, Phys. Lett. **78B**, 492 (1978); Z. Phys. C **2**, 117 (1979).

[3] M. J. Savage and R. P. Springer, Phys. Rev. D **42**, 1527 (1990).

[4] S. M. Sheikholeslami, M. P. Khanna, and R. C. Verma, Phys. Rev. D **43**, 170 (1991).

[5] Y. Kohara, Phys. Rev. D **44**, 2799 (1991).

[6] B. Guberina, D. Tadić, and J. Trampetić, Z. Phys. C **13**, 251 (1982).

[7] F. Hussain and M. D. Scadron, Nuovo Cimento **79A**, 248 (1984); F. Hussain and K. Khan, *ibid.* **88A**, 213 (1985).

[8] D. Ebert and W. Kallies, (a) Phys. Lett. **131B**, 183 (1983); **148B**, 502(E) (1984); (b) Yad. Fiz. **40**, 1250 (1984) [Sov. J. Nucl. Phys. **40**, 794 (1984)]; (c) Z. Phys. C **29**, 643 (1985).

[9] H. Y. Cheng, Z. Phys. C **29**, 453 (1985).

[10] Yu. L. Kalinovsky, V. N. Pervushin, G. G. Takhtamyshev, and N. A. Sarikov, Fiz. Elem. Chastits At. Yadra **14**, 77 (1988) [Sov. J. Part. Nucl. **14**, 47 (1988)], and references therein.

[11] S. Pakvasa, S. F. Tuan, and S. P. Rosen, Phys. Rev. D **42**, 3746 (1990).

[12] G. Kaur and M. P. Khanna, Phys. Rev. D **44**, 182 (1991).

[13] G. Turan and J. O. Eeg, Z. Phys. C **51**, 599 (1991).

[14] S. Rudaz and M. Voloshin, Phys. Lett. B **252**, 443 (1990); A. Acker, S. Pakvasa, S. F. Tuan, and S. P. Rosen, Phys. Rev. D **43**, 3083 (1991); T. Mannel, W. Roberts, and Z. Ryzak, Phys. Lett. B **255**, 593 (1991); **259**, 485 (1991); Nucl. Phys. **B355**, 98 (1991).

[15] N. G. Deshpande, J. Trampetić, and A. Soni, Mod. Phys. Lett. A **3**, 749 (1988).

[16] M. Jarfi *et al.*, Phys. Rev. D **43**, 1599 (1991).

[17] R. E. Marshak, Riazuddin, and C. P. Ryan, *Theory of Weak Interactions in Particle Physics* (Wiley Interscience, New York, 1969).

[18] We follow the notation of J. Bjorken and S. Drell, *Relativistic Quantum Mechanics* (McGraw-Hill, New York, 1964) except that our γ_5 is of opposite sign to theirs.

[19] See, e.g., D. Bailin, *Weak Interactions* (Sussex University Press, Sussex, 1977).

[20] The widely employed formula

$$B^{CA}=-\frac{\sqrt{2}}{f_P}(m_i+m_f)\sum_{B_n}\left[\frac{g_A^{B_fB_n}a_{ni}}{m_i-m_n}+\frac{a_{fn}g_A^{B_iB_n}}{m_f-m_n}\right]$$

for the p-wave amplitude does not take into account the contribution (though small) due to $(M_{fi}-i\sqrt{2}/f_P q_\mu T^\mu)$ evaluated in the $q_\mu \to 0$ limit.

[21] H. Y. Cheng, Int. J. Mod. Phys. A **4**, 495 (1989).

[22] D. Tadić and J. Trampetić, Phys. Lett. **114B**, 179 (1982); A. J. Buras, J.-M. Gérard, and R. Rückl, Nucl. Phys. **B268**, 16 (1986).

[23] A. Chodos, R. L. Jaffe, K. Johnson, and C. B. Thorn, Phys. Rev. D **10**, 2599 (1974); T. DeGrand, R. L. Jaffe, K. Johnson, and J. Kiskis, *ibid.* **12**, 2060 (1975).

[24] The PC matrix elements a_{ij} were expressed before [6,9] in terms of the bag overlap integrals a, b, and c, which are related to X_1 and X_2 by $X_1=(-b+c)/4\pi$ and $X_2=(a+c)/4\pi$. Note that the sign of our $a_{\Sigma_c^0\Lambda}$ is opposite to that given in Ref. [9] owing to a different convention for our baryon wave functions [see Eq. (A10)].

[25] Particle Data Group, J. J. Hernández *et al.*, Phys. Lett. B **239**, S1 (1990).

[26] R. Pérez-Marcial, R. Huerta, A. García, and M. Avila-Aoki, Phys. Rev. D **40**, 2955 (1991); **44**, 2203(E) (1991).

[27] N. Isgur and M. Wise, Phys. Lett. B **232**, 113 (1989); **237**, 527 (1990).

[28] M. Avila-Aoki, A. García, R. Huerta, and R. Pérez-Marcial, Phys. Rev. D **40**, 2944 (1989).

[29] H. Albrecht *et al.*, Phys. Lett. B **269**, 234 (1991).

[30] S. Barlag *et al.*, Z. Phys. C **48**, 29 (1990).

[31] P. Avery *et al.*, Phys. Rev. D **43**, 3599 (1991).

[32] D. Izatt and C. Detar, Nucl. Phys. **B199**, 269 (1982).

[33] M. Procario, Report No. CMU-HEP-91-12, 1991 (unpublished).

[34] P. Avery *et al.*, Phys. Rev. Lett. **65**, 2842 (1990).

[35] H. Albrecht *et al.*, Phys. Lett. B **274**, 239 (1992).

[36] In contrast with Ref. [9], we find a destructive interference between B^{pole} and B^{fac} for the p-wave amplitude of $\Lambda_c^+ \to \Lambda\pi^+$. This is attributed to the fact that this time we have applied the wave functions of the baryons given by Eq. (A10) consistently to the baryon matrix elements and to coupling constants.

[37] The parameter c_2 is related in Ref. [12] to the Wilson coefficients c_+ and c_- by $c_2=(c_- - c_+)/2$, which is of opposite sign to our c_2 in Eq. (2.20).

[38] J. M. Weiss, in *Baryon 1980,* Proceedings of the 4th International Conference on Baryon Resonances, Toronto, Canada, 1980, edited by N. Isgur (University of Toronto, Toronto, 1980).

[39] M. Basile *et al.*, Nuovo Cimento **62A**, 14 (1981).

[40] H. Albrecht *et al.*, Phys. Lett. B **207**, 109 (1988).

[41] J. Körner and M. Kramer, Report No. MZ-TH/91-07, 1991 (unpublished), quoted in Ref. [1].

[42] T. A. DeGrand and R. L. Jaffe, Ann. Phys. (N.Y.) **100**, 425 (1976).

[43] T. A. DeGrand, Ann. Phys. (N.Y.) **101**, 496 (1976).

[44] C. Leroy, Phys. Rev. D **18**, 326 (1978); S. Tatur, *ibid.* **20**, 2972 (1979).

[45] However, it should be stressed that the excited $P_{3/2}$ quark states are not considered in Ref. [13].

[46] See, e.g., V. B. Berestetskii, E. M. Lifshitz, and L. P. Pitaevskii, *Relativistic Quantum Theory* (Pergamon, Oxford, 1971).

[47] G. Campbell, Jr., Phys. Rev. D **13**, 662 (1976).

[48] M. P. Khanna and R. C. Verma, Z. Phys. C **47**, 275 (1990).

[49] The generalized GT relation given by Eq. (D3) is valid for $P=P^a$ $(a=1,\ldots,8)$ in the SU(3) representation. For kaons and the charged pions, one has $g_{B^*BP}=(m_{B^*}-m_B)g^A_{B^*B}/f_P$; see also M. Milosović, D. Tadić, and J. Trampetić, Nucl. Phys. **B207**, 461 (1982).

[50] S. Pakvasa and J. Trampetić, Phys. Lett. **126B**, 122 (1983).

[51] I. Picek, D. Tadić, and J. Trampetić, Nucl. Phys. **B177**, 382 (1981).